

Cite this: *Chem. Soc. Rev.*, 2014, 43, 6141

## A supermolecular building approach for the design and construction of metal-organic frameworks

Vincent Guillerm,<sup>a</sup> Dongwook Kim,<sup>b</sup> Jarrod F. Eubank,<sup>c</sup> Ryan Luebke,<sup>a</sup> Xinfang Liu,<sup>b</sup> Karim Adil,<sup>a</sup> Myoung Soo Lah<sup>\*b</sup> and Mohamed Eddaoudi<sup>\*ad</sup>

In this review, we describe two recently implemented conceptual approaches facilitating the design and deliberate construction of metal-organic frameworks (MOFs), namely supermolecular building block (SBB) and supermolecular building layer (SBL) approaches. Our main objective is to offer an appropriate means to assist/aid chemists and material designers alike to rationally construct desired functional MOF materials, made-to-order MOFs. We introduce the concept of **net**-coded building units (**net**-cBUs), where precise embedded geometrical information codes uniquely and matchlessly a selected net, as a compelling route for the rational design of MOFs. This concept is based on employing pre-selected 0-periodic metal-organic polyhedra or 2-periodic metal-organic layers, SBBs or SBLs respectively, as a pathway to access the requisite **net**-cBUs. In this review, inspired by our success with the original **rht**-MOF, we extrapolated our strategy to other known MOFs via their deconstruction into more elaborate building units (namely polyhedra or layers) to (i) elucidate the unique relationship between edge-transitive polyhedra or layers and minimal edge-transitive 3-periodic nets, and (ii) illustrate the potential of the SBB and SBL approaches as a rational pathway for the design and construction of 3-periodic MOFs. Using this design strategy, we have also identified several new hypothetical MOFs which are synthetically targetable.

Received 22nd April 2014

DOI: 10.1039/c4cs00135d

[www.rsc.org/csr](http://www.rsc.org/csr)

### 1. Introduction

Over the past two decades, the research community has witnessed the prominent growth of a special class of materials, namely metal-organic frameworks (MOFs), that have risen to the forefront of solid-state chemistry.<sup>1,2</sup> This particular class of crystalline materials offers a high degree of structural and functional tunability<sup>3,4</sup> that is not available with other conventional porous materials (*e.g.*, zeolites, activated carbons).<sup>2</sup> The resultant structural modularity (*e.g.*, use of different metals, reticular chemistry,<sup>5</sup> post-synthetic modifications,<sup>6</sup> *etc.*) and exceptional controlled porosity make MOFs ideal candidate materials to

address many enduring societal challenges pertaining to energy and environmental sustainability and beyond.<sup>7,8</sup>

MOF crystal chemistry offers the potential to introduce desired properties and functionality prior to the assembly process by pre-selecting building blocks to contain desired structural and geometrical information that codes for a given underlying net. The aforementioned assembly process, referred to as the molecular building block (MBB) approach, permits access to MOFs with simple topologies, such as edge-transitive nets (nets with one kind of edge).<sup>1</sup> The successful implementation of the MBB approach for the rational design and construction of MOFs necessitates the satisfaction of key prerequisites: (1) selection of an ideal blueprint net that is exclusive for the assembly of its corresponding basic building units, and (2) isolation of the reaction conditions that consistently allow the *in situ* formation of the desired inorganic MBB, matching the augmented basic building units (vertex figures) of the targeted net. Notably, uninodal and binodal nets with high connectivity, that is having at least one node with connectivity  $n > 8$ , are suitable targets in crystal chemistry, as they offer a limited number of plausible nets for the assembly of their related highly-connected MBBs.<sup>9</sup>

The difficulty in isolating reaction conditions that permit the formation of highly-connected MBBs (*i.e.*,  $\geq 12$ ) is directly evident by the relatively scarce number of MOFs with high connectivities.<sup>10-19</sup>

<sup>a</sup> Functional Materials Design, Discovery and Development (FMD<sup>3</sup>), Advanced Membranes and Porous Materials Center, Division of Physical Sciences and Engineering, King Abdullah University of Science and Technology (KAUST), Thuwal 23955-6900, Kingdom of Saudi Arabia.

E-mail: [mohamed.eddaoudi@kaust.edu.sa](mailto:mohamed.eddaoudi@kaust.edu.sa)

<sup>b</sup> Department of Chemistry, Ulsan National Institute of Science and Technology, Ulsan, 689-798, Korea. E-mail: [mslah@unist.ac.kr](mailto:mslah@unist.ac.kr); Fax: +82-52-217-2019; Tel: +82-52-217-2931

<sup>c</sup> Department of Chemistry and Physics, Florida Southern College, Lakeland, FL 33801, USA

<sup>d</sup> Department of Chemistry, University of South Florida, 4202 East Fowler Avenue, Tampa, FL 33620, USA



It should be mentioned that simple MBBs with connectivity of 8 or greater are often too intricate to be systematically obtained by means of simple organic ligands or polynuclear clusters. Nonetheless, such complex and elaborate building blocks can be designed and attained as supermolecular building blocks (SBBs), larger building units based on the assembly of relatively simple and readily accessible (typically) 3- or 4-connected (3-c or 4-c) MBBs. Utilization of these SBBs with a high degree of symmetry and connectivity, as well as the needed elaborate directional and structural information, permits access to novel MOF platforms, as recently demonstrated by the use of 24-, 18-, or 12-connected metal-organic polyhedra (MOPs) as SBBs for the intended formation of highly-connected **rht**-MOFs,<sup>12,13,20,21</sup> **gea**-MOFs,<sup>10</sup> and **fcu**-MOFs, respectively.<sup>22,23</sup>

The aforementioned SBB approach calls for utilization of MOPs as SBBs in the construction of MOFs, an approach with

great potential to enhance control over the targeted framework.<sup>12,24</sup> In this approach, the SBB, formed *in situ* through association of MBBs, is employed as a building unit with larger dimensions and more complex connectivity.<sup>12</sup> In general, when constructing MOFs from SBBs the peripheral points of extension of the SBB define a geometric building unit that is equivalent to augmenting a node in a network, a net vertex figure. Programming the SBB with a hierarchy of proper information to promote the synthesis of targeted structures, while simultaneously avoiding other easily attainable low-connectivity nets,<sup>25,26</sup> represents a significant advancement in framework design.<sup>10</sup>

Evidently, the more directional and structural information that can be incorporated into the building unit, the higher the degree of predictability and potential for design. Of special interest in crystal chemistry are minimal edge-transitive 3-periodic nets—a net with only one or two kinds of edges—enclosing



**Vincent Guillerm**

*Vincent Guillerm was born in Morlaix, France. He obtained his MSc from the Université de Rennes I, France (2007), and his PhD in solid state chemistry from the Université de Versailles Saint-Quentin-en-Yvelines, France (2011), under the supervision of Dr Christian Serre. He is currently a Postdoctoral fellow at the King Abdullah University of Science and Technology (KAUST, Kingdom of Saudi Arabia) in Prof. Mohamed Eddaoudi's Functional Materials*

*Design Discovery and Development (FMD<sup>3</sup>) Research group, Advanced Membranes and Porous Materials Center. His current work covers the rational design, synthesis, functionalization of MOFs, porous organic polymers for sorption related applications (storage, separation...).*



**Dongwook Kim**

*Dongwook Kim was born in Korea in 1985. He received his bachelor's degree in Chemistry from Hanyang University, Korea, in 2011. He is doing his PhD degree at Department of Chemistry, Ulsan National Institute of Science and Technology under the supervision of Prof. Myoung Soo Lah. He is currently working on the preparation of MOFs based on MOPs as supermolecular building blocks and studying their various properties including gas sorption behaviors.*



**Jarrod F. Eubank**

*Jarrod F. Eubank was born in Sturgis, Kentucky, USA (1980). He received his BS from Western Kentucky University (2002), and his PhD from the University of South Florida (2008) with Professor Mohamed Eddaoudi. He was a CNRS Postdoctoral Fellow at Université de Versailles Saint-Quentin-en-Yvelines with professors Gérard Férey and Christian Serre (2008–2010). He is currently Visiting Assistant Professor in the Department of Chemistry and Physics at*

*Florida Southern College. His current research focuses on the design, synthesis, and applications, especially biological, of MOFs and other related materials.*



**Ryan Luebke**

*Ryan Luebke was born in Madison, Wisconsin, USA. He received his BSc in Chemistry (2004) and MBA (2007) from the University of South Florida in Tampa, Florida. He is currently working towards his PhD in Chemical Science at King Abdullah University of Science and Technology (KAUST) under the supervision of Professor Mohamed Eddaoudi. His research focuses on the design and synthesis of MOFs for gas separation and storage.*



edge-transitive polyhedra or layers as hierarchical building units that are distinctively coding for the associated net.

Inspired by our success with the design of the original **rht**-MOF, we extrapolated our strategy to other known MOFs *via* their deconstruction into more elaborate building units, namely polyhedra; we took the strategy one step further, and explored other potential elaborate building units, namely metal-organic layers, resulting in the realization of the analogous supermolecular building layer (SBL) approach. The combined efforts allowed us to (i) elucidate the unique relationship between edge-transitive polyhedra or layers and minimal edge-transitive 3-periodic nets, and (ii) illustrate the potential of the SBB and SBL approaches as rational pathways for the design and construction of 3-periodic MOFs. In this review, we introduce the concept of **net**-coded building units (**net**-cBUs), where precise embedded geometrical information codes uniquely and matchlessly a select net, as a compelling route for the rational design of MOFs. This concept is based on employing pre-selected 0-periodic metal-organic polyhedra or 2-periodic metal-organic layers, SBBs or SBLs respectively, as a pathway to access the requisite **net**-cBUs.

In this review, we will enumerate the most notable MOFs comprised of MOPs, obtained either by serendipity or designed through the powerful SBB approach, as well as another class of MOFs that are built from simple or highly elaborate pillaring of layers, some recently designed *via* the SBL approach. This review focuses on selected examples that can be rationally designed *via* the unique supermolecular building approaches, rather than presenting an exhaustive catalog. For detailed analysis of network topologies and their corresponding basic vertex connectivities, we suggest the reader to refer to seminal work by O'Keeffe and Yaghi, *et al.*<sup>27–29</sup>

Markedly, our aim is to provide the material designers the required tools permitting the access to and practice of the SBB and the SBL approaches for the rational design and construction of MOFs, tailored for specific applications. Accordingly, this review is divided into two parts: The first section includes a list of pre-programmed MOPs, as well as various ways for their subsequent cross-linking into targeted specific net topologies; in the second part, the SBL approach will be detailed, offering the kind of layers that can be targeted and enumerating the various possibilities for their subsequent pillaring.

## 2. Supermolecular building blocks (SBBs)

The SBB approach relies on the use of a MOP as an elaborate building entity, coded to contain the requisite information to construct a targeted MOF with a given topology. For this purpose, the MOP must contain the geometrical information and desired peripheral points of extension (connectivity) that match the **net**-cBUs, which codes uniquely for a select targeted net.

Our groups demonstrate that it is possible to utilize externally functionalized MOPs as SBBs for the synthesis of MOFs with unique and predictable nets.<sup>13,23,24</sup> The SBB approach, conceived and introduced by Eddaoudi's group,<sup>24</sup> is well-positioned to address the enduring scarcity of highly-connected building units required to construct MOFs based on high-connectivity nets. Indeed, simple MBBs with connectivity of 8 or greater are often too intricate to systematically obtain by means of simple organic ligands or multi-nuclear clusters. Such complex structures can be more easily



**Myoung Soo Lah**

where he is presently a professor of department of chemistry. He is interested in the development of metal-organic systems such as MOPs and MOFs for the applications in the areas of storage, capture/separation, and catalysis.

*Myoung Soo Lah attended Seoul National University, Korea, for his BSc and MSc and earned his PhD in chemistry from the University of Michigan, Ann Arbor, in 1991. After his postdoctoral research in protein crystallography from the same university, he became a faculty member of the department of chemistry, Hanyang University in 1992 and then moved to Ulsan National Institute of Science and Technology in 2010,*



**Mohamed Eddaoudi**

*Mohamed Eddaoudi was born in Agadir, Morocco. He is currently Professor of Chemical Science and Associate Director of the Advanced Membranes and Porous Materials Center, King Abdullah University of Science and Technology (KAUST, Kingdom of Saudi Arabia). He received his PhD in Chemistry, Université Denis Diderot (Paris VII), France. After postdoctoral research (Arizona State University, University of Michigan), he started his independent academic career as Assistant Professor, University of South Florida (2002), Associate Professor (2008), and Professor (2010). His research focuses on developing strategies, based on (super)-molecular building approaches (MBB, SBB, SBL), for rational construction of functional solid-state materials, namely MOFs. Their prospective uses include energy and environmental sustainability applications. Dr Eddaoudi's eminent contribution to the burgeoning field of MOFs is evident by his selection in 2014 as a Thomson Reuters Highly Cited Researcher.*



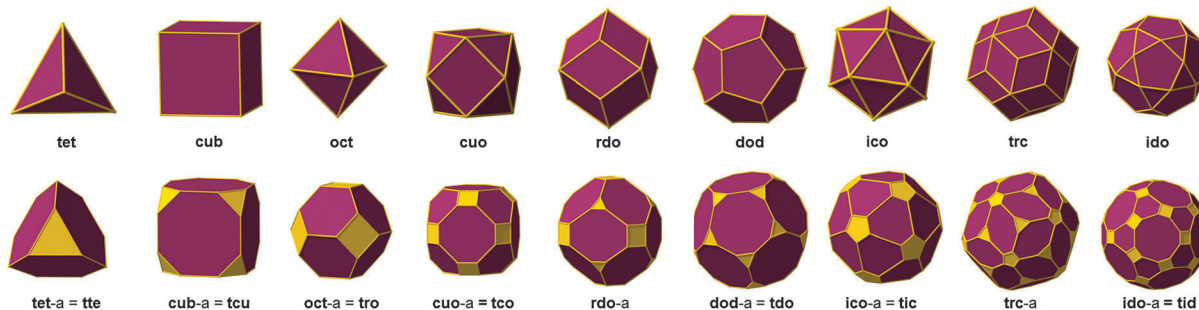


Fig. 1 The nine edge-transitive polyhedra (top) and their augmented (i.e., truncated) equivalents.

designed by utilizing SBBs with a high degree of symmetry and connectivity; consequently, enhanced directional and structural information is available for the SBB. In principle, there is a degree of predictability in such a strategy that is not present with low-connectivity basic MBBs, thus novel structures can be targeted. Practically, highly-connected nets with at least one node  $\geq 12$  are suitable targets in crystal chemistry, as they limit the number of outcome nets for the assembly of their associated highly-connected building blocks. Additionally, selection of blueprint nets based on minimal edge-transitive 3-periodic nets offers great potential for the rational design and construction of MOFs.

Fascinatingly, there exist only nine polyhedra that are edge-transitive. This feature is of prime importance in crystal chemistry as their augmented (truncated) polyhedron can be ideally employed as a polyhedron-blueprint to target the associated MOP and their subsequent assembly into related MOFs. Fig. 1 shows the edge-transitive polyhedra along with their derived truncated polyhedra. A closer look at these edge-transitive polyhedra reveals that seven out of nine are constructed exclusively from 3-c nodes, 4-c nodes or a combination of 3-c and 4-c nodes (i.e., **tet**, **cub**, **oct**, **cuo**, **rdo**, **dod**, and **ido**). Markedly, the three edge-transitive polyhedra (i.e., **oct**, **cuo**, **ido**) based on 4-c nodes have a similar corresponding square vertex figure, and are ideal targets in crystal chemistry for the construction of MOPs. That is, there are only three ways to link squares with one kind of edge into a polyhedron. It is to be mentioned that a vertex figure in a given polyhedron defines the points at which the MBBs are joined together to form the associated MOP (Fig. 2).

The requisite inorganic 4-connected square MBBs are readily accessible *via* metal-ligand directed coordination chemistry. This is exemplified by the dinuclear square paddlewheel cluster occurring with various metals (Ru, Cu, Rh, No, Fe, Ni, Co, Re, Cr, Zn, Mn, W, Tc, Os, Bi, Rh/Bi, Pt, Al, Mg, In, Pd/Co, Pd/Mn, Pd/Zn).<sup>30</sup> The paddlewheel-shaped MBB offers access to a plethora of structures,<sup>31</sup> due to its relatively low connectivity (4-c or 6-c, typically); its combination with organic ligands has been extensively studied and some synthetic conditions are already well-established permitting access to the aforementioned MBB *in situ*, and its transposition into specific structural motifs.

## 2.1. Metal-organic polyhedra (MOPs)

**2.1.1. Influence of the bent ligands.** Most of the reported MOPs are constructed by the assembly of inorganic MBBs, single-metal ions or clusters (M), with bent ligands (L), as exemplified by

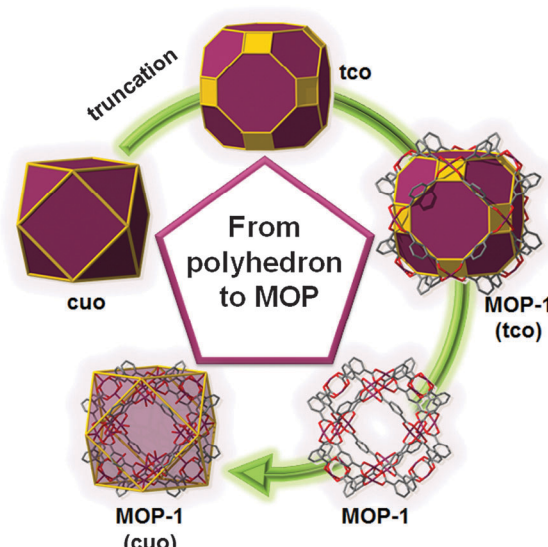


Fig. 2 Schematic showing the relation between the edge-transitive cuboctahedron and the copper-isophthalate MOP-1.

Fujita *et al.* through their exemplary work, over the past decade, with palladium-based MOPs, which confirms the importance of the geometry or bent angle of the ligand (Fig. 3).<sup>32,33</sup> By a slight variation of the bent angle, they were able to isolate the experimental frontier angle between two kinds of MOPs ( $M_{12}L_{24}$  and  $M_{24}L_{48}$ ) both with the same 1:2 M to L ratio. Interestingly, the  $M_{24}L_{48}$  MOP obtained can be regarded as a rhombicuboctahedron, which is not an edge-transitive polyhedron. The expected edge-transitive MOP for the assembly of squares with bent ligands having angles in the range of 134–149° should have been an  $M_{30}L_{60}$  **ido**-MOP (with an ideal bent angle of 144°). This finding reveals the capability of isolating additional closely-related MOPs that could each offer potential for the rational design and construction of MOFs. Along the same line, since the first use of the name metal-organic polyhedron and the abbreviation of MOP, with the report of Cu-paddlewheel-based MOP-1,<sup>34,35</sup> exploration of similar systems based on paddlewheels (Mo, Cu, *etc.*) linked through dicarboxylate-based ligands has led to the isolation of several MOPs ( $M_2L_4$ ,  $M_3L_6$ ,  $M_6L_{12}$ ,  $M_{12}L_{24}$ ) by varying the bent angles of the ligands from 0 to 120°.<sup>36–38</sup>

Furthermore, the possibility for synthesis of expanded MOPs has been demonstrated, either by extending the lengths of a ligand,<sup>39</sup> or by the incorporation of ligands with various angles



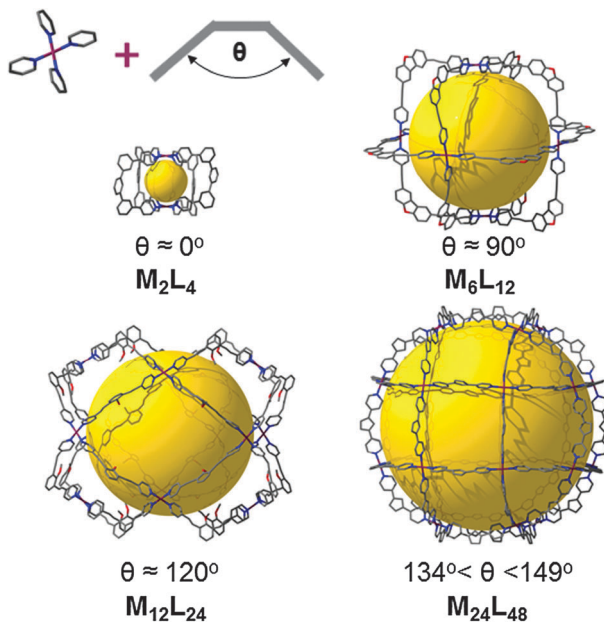


Fig. 3 Illustration of the strong influence of the bent angle of the ligand on the geometry of the resulting MOP.

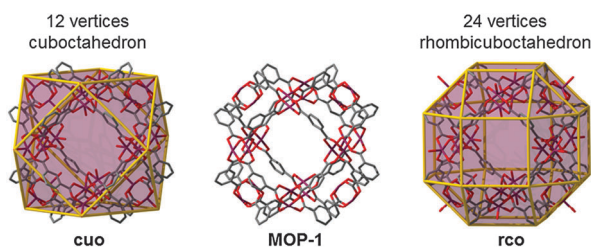


Fig. 4 Depending on the chosen vertices, MOP-1 can be regarded as a cuboctahedron, **cuo** (12 paddlewheels as vertices), or a rhombicuboctahedron, **rco** (24 bent ligands as vertices).

in the same polyhedron.<sup>40</sup> This mixed-ligand strategy allows the discovery of more complex and finely-tailored MOPs that can surely be used *in fine* for the formation of very complex extended structures.<sup>10</sup> For a more complete overview of the fascinating MOP structures, the reader is invited to read the excellent and well-documented reviews of Stang *et al.*<sup>41,42</sup> and Zaworotko *et al.*<sup>43</sup>

**2.1.2. Versatile MOPs.** MOPs constructed from specific versatile MBBs, such as the di-copper paddlewheel, include the previously mentioned and already well-known MOP-1.<sup>34,35</sup> Specifically, MOP-1 can be regarded as a cuboctahedron, when the functionalizable apical positions of the paddlewheels are considered as the vertices of the polyhedron. It can alternatively be regarded as a rhombicuboctahedron with 24 vertices when considering the 5-position of the isophthalates as vertices of the polyhedron. The same principles are, of course, applicable to other paddlewheel-based MOPs (Fig. 4), allowing, *in fine*, numerous design options.

## 2.2. MOPs for MOF design

**2.2.1. Assembly of tetrahedral SBBs.** Aside from the previous examples, numerous other types of MOPs are targetable, and potentially can be utilized as SBBs to target 3-periodic MOFs. Several examples of MOPs which could be envisioned as tetrahedral SBBs have been published. In 2005, Yaghi *et al.* reported the synthesis of various sulfate-capped discrete tetrahedral MOPs (IRMOP-51 to -53) based on the assembly of linear and triangular ligands with Fe-based trinuclear clusters, trimers.<sup>44</sup> The vertices of each member of this IRMOP series are composed of  $\text{Fe}_3\text{O}(-\text{O}_2\text{CR})_3(\text{SO}_4)_3(\text{py})_3$  units with the sulfates acting as capping groups that prevent the formation of extended structures. Thus, the  $\text{Fe}_3\text{O}(-\text{O}_2\text{CR})_3$  unit acts as a triangular MBB that is connected to three ditopic (IRMOP-50 to -53) organic linkers. In all cases the coordination sphere of each metal is completed by a terminal pyridine ligand that gives an overall octahedral

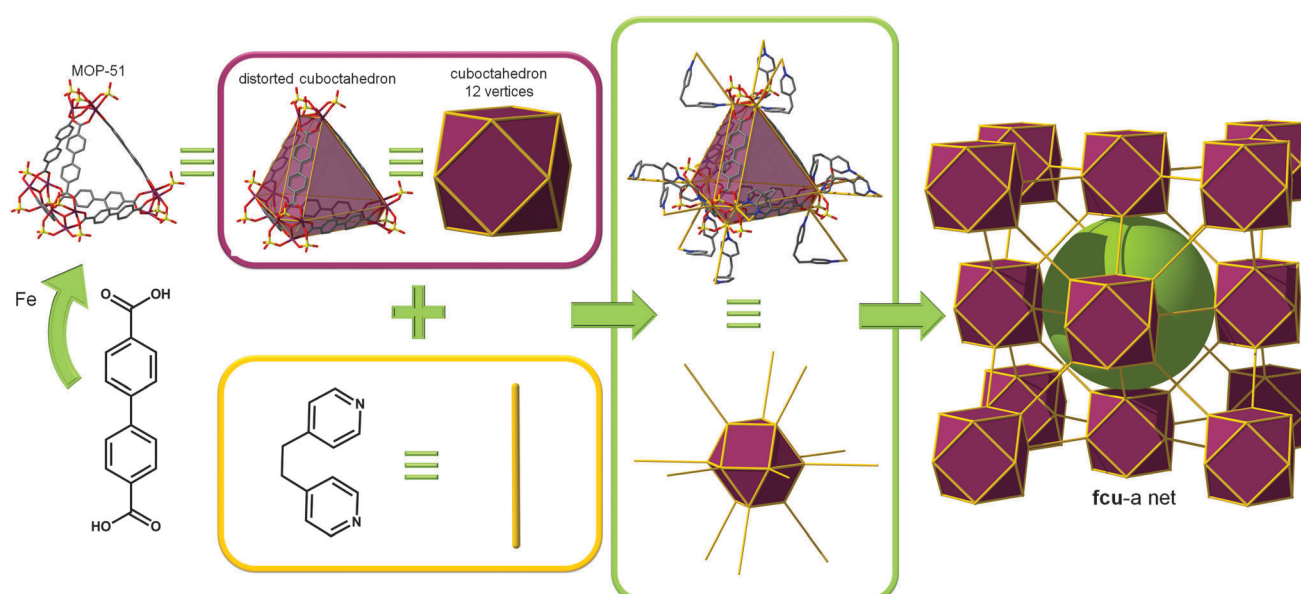


Fig. 5 The bridging of MOP-51 SBBs by twelve 2-c ligands leads to MOF-500 with **fcu** topology.

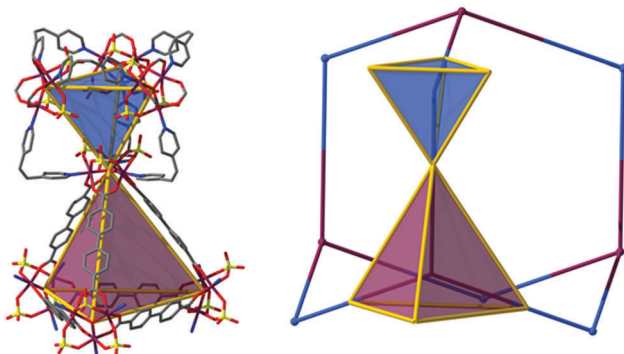


Fig. 6 MOF-500 can be regarded as the assembly of two distinct tetrahedral cages. In this case, the resulting topology is **dia** (or **dia-b-e**).

Fe center. Shortly thereafter, they demonstrated the possibility to connect these MOPs using *cis*-1,2-bis-4-pyridylethane (BPE), instead of pyridine, to produce MOF-500 (Fig. 5).<sup>45</sup> In fact, the crystal structures of MOF-500 and cubic IRMOP-51 are superimposable and have the same  $F\bar{4}3m$  symmetry; contractions of only 0.4 Å between adjacent tetrahedra in IRMOP-51 are required for connection to occur in MOF-500.

While considering the structure of MOF-500 as bridging of MOP-51 (distorted cuboctahedron, 12 points of extension) through 2-c ligands, the structure can be defined as having **fcu** topology. However this net can also be regarded as **crs** topology with a  $[\text{Fe}_3\text{O}(\text{SO}_4)_3(-\text{O}_2\text{CR})_3(\text{py})_3]$  unit as a uninodal 6-c MBB, where the MBBs form two different kinds of corner-shared tetrahedral MOPs in a staggered fashion (Fig. 6). In the network, the 6-c  $[\text{Fe}_3\text{O}(\text{SO}_4)_3(-\text{O}_2\text{CR})_3(\text{py})_3]$  MBB of  $C_{3v}(3m)$  point symmetry is interconnected *via* three 2-c BPDC ligands (where,  $\text{H}_2\text{BPDC} = 4,4'$ -biphenyldicarboxylic acid) and three 2-c BPE ligands. Four MBBs are interconnected *via* six BPDC ligands to form a tetrahedral MOP and other four 6-c MBBs are similarly interconnected *via* six BPE ligands to another tetrahedral MOP. These two different kinds of tetrahedral MOPs are corner-shared in a staggered fashion and the topology of the network is a **dia-b-e** (an edge net of **dia-b** (binary **dia**)). It is worth mentioning that **dia** (diamond) is the default (most commonly occurring) net for the assembly of tetrahedra.

Férey *et al.* reported a key contribution based on corner-shared tetrahedral SBBs, resulting in the discovery of mesoporous MOFs having a zeolite topology; at the time of their discovery these MOFs had some of the highest specific surface areas reported. These unique MOFs, namely MIL-100 and MIL-101, are based on the self-assembly of similar metal-organic supertetrahedra (STs).<sup>46–48</sup> The arrangement of organic linkers, respectively 1,3,5-benzenetricarboxylate (1,3,5-BTC; trimesate) and 1,4-benzenedicarboxylate (1,4-BDC; p-BDC, terephthalate), and inorganic trimers leads to the formation of a large ST. The ST is built in such a way that the four vertices of the ST are occupied by trimers while the organic linkers are located at the four faces or six edges of the ST. The connection of STs is established through vertices to ensure a 3-periodic network of corner-shared tetrahedral SBBs. When considering the assembly of these STs in MIL-100 and MIL-101, the MOFs exhibit the same topology (**mtn**) related to the **MTN** zeolite, but a precise analysis of points of extension

reveals an important difference. Despite the fact that both have 12 points of extension, an ST built up from inorganic trimers ( $\text{M} = \text{Cr, Fe, Al, etc.}$ ) and the 2-c 1,4-BDC (MIL-101) possesses vertices which match those from a truncated tetrahedron, while an ST built from the same types of inorganic trimers but with the 3-c 1,3,5-BTC ligand (MIL-100) can be regarded as a distorted cuboctahedron. This difference is of prime importance as it exemplifies the possibility of using STs as SBBs for synthesizing structurally-related MOFs.

Indeed, Serre and co-workers have recently reported a novel mesoporous MOF, MIL-143, synthesized using a mixed-ligand strategy. MIL-143 is built up from two kinds of STs (the one from MIL-101, and a benzene-tribenzoate (BTB) expansion of the ST from MIL-100).<sup>49</sup> From a topological point of view, this structure can be interpreted in several different ways (Fig. 7). The first one is to consider the truncated tetrahedron STs (composed of six linear 1,4-BDC ligands) as the SBBs; which, when connected through the triangular BTB ligands leads to the binodal (3,12)-c network with **ttt** topology. Alternatively, if the expanded STs (with BTB on the faces) are considered as the SBBs, they are then linked through the linear 1,4-BDC ligands, which results in the interpretation of the structure as the well-known **fcu** topology. Both **fcu** and **ttt** are edge-transitive nets, therefore the obtained structures are those with the higher probability to form. Similarly to MOF-500, these MOPs can be considered as tetrahedra, which are corner-shared in a staggered fashion, and the topology of the network is **dia-b-e**. This is actually the only way for linking corner-shared staggered tetrahedra with a 180° angle.

Thus, the use of tetrahedral SBBs can provide access to diamond topologies, diamond-related topologies, and the zeolitic **mtn** topology. In fact, Férey and coworkers have shown the potential to construct other MOFs related to additional zeolitic topologies through molecular modelling of hypo-MIL-1 and hypo-MIL-2.<sup>50</sup>

**2.2.2. Assembly of cubic SBBs.** Metal-organic cubes (MOCs) are another category of MOPs that offer potential to serve as SBBs, as first reported by Eddaoudi *et al.* in 2004.<sup>25</sup> The architecture of this particular MOP consists of heterofunctional imidazoledicarboxylate ligands bridging eight single-metal ions, and, when considering the functionalized periphery, can be viewed as a double four-membered ring (d4R) composite building unit (as in conventional zeolites), *i.e.*, a building unit consisting of eight tetrahedra in a cube-like arrangement where the ligands replace the edges of the cube and the vertices offer potential for cross-linking. The use of such MOPs as programmed building blocks with a hierarchy of appropriate information enables and promotes the synthesis of targeted structures, while simultaneously avoiding other easily attainable or default 4-connected nets, such as the aforementioned diamond net (**dia**).<sup>51</sup>

**Vertex-linked MOCs.** Eddaoudi *et al.* reported the utilization of these MOCs as SBBs, highlighting the ability to cross-link them into 3-periodic MOF structures with zeolite-like topologies, *i.e.*, zeolite-like metal-organic-frameworks (ZMOFs). The ZMOFs could be constructed by linking these MOCs *via* linear links, thus giving rise to MOFs having **lta**<sup>26</sup> or **aco**<sup>52</sup> (also known as **pcb**) topologies (Fig. 8). Alternatively, linking these MOCs through 4-c nodes should result in ZMOFs having **ast** (Fig. 8)<sup>26</sup> or **asv** topologies.



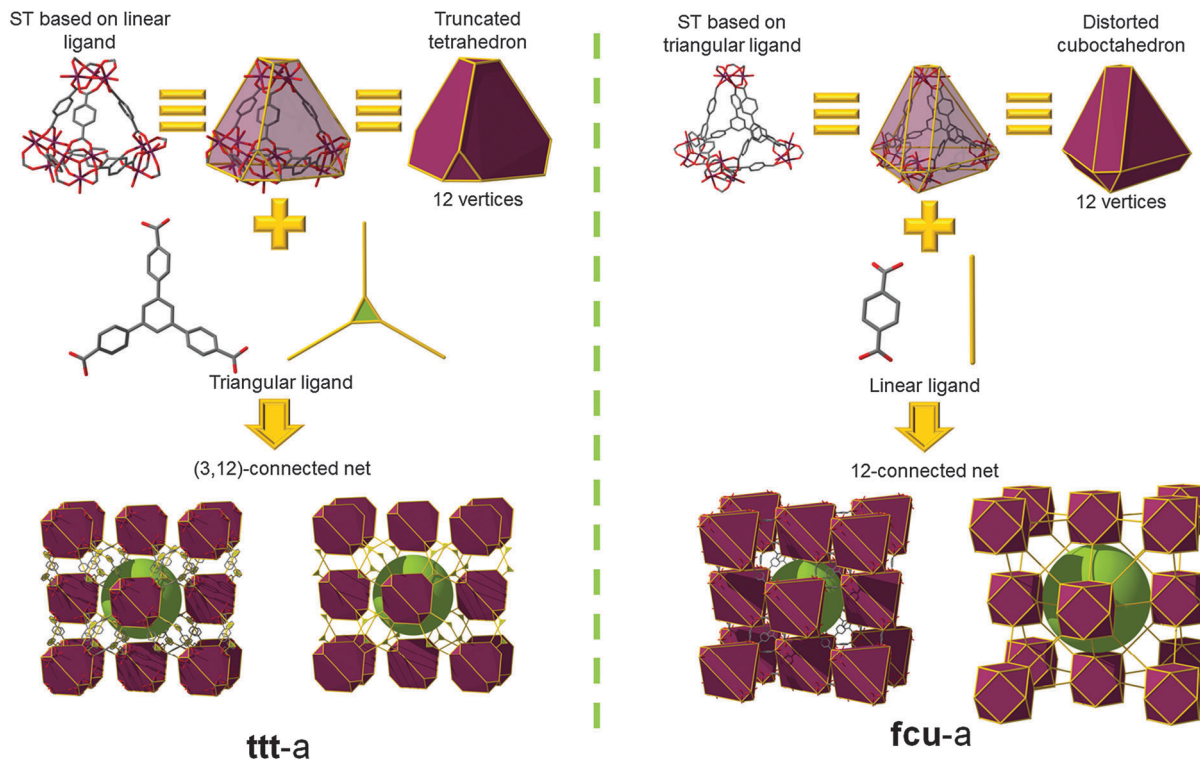


Fig. 7 Topological analysis of MIL-143. Considering the SBBs as truncated tetrahedra constructed from 1,4-BDC and Fe trimers, crosslinked by BTB ligands, the topology is **ttt**. Considering the SBBs as distorted cuboctahedra constructed from BTB and Fe trimers, bridged by 1,4-BDC ligands, the topology is **fcu**. Both **fcu** and **ttt** are edge-transitive nets.

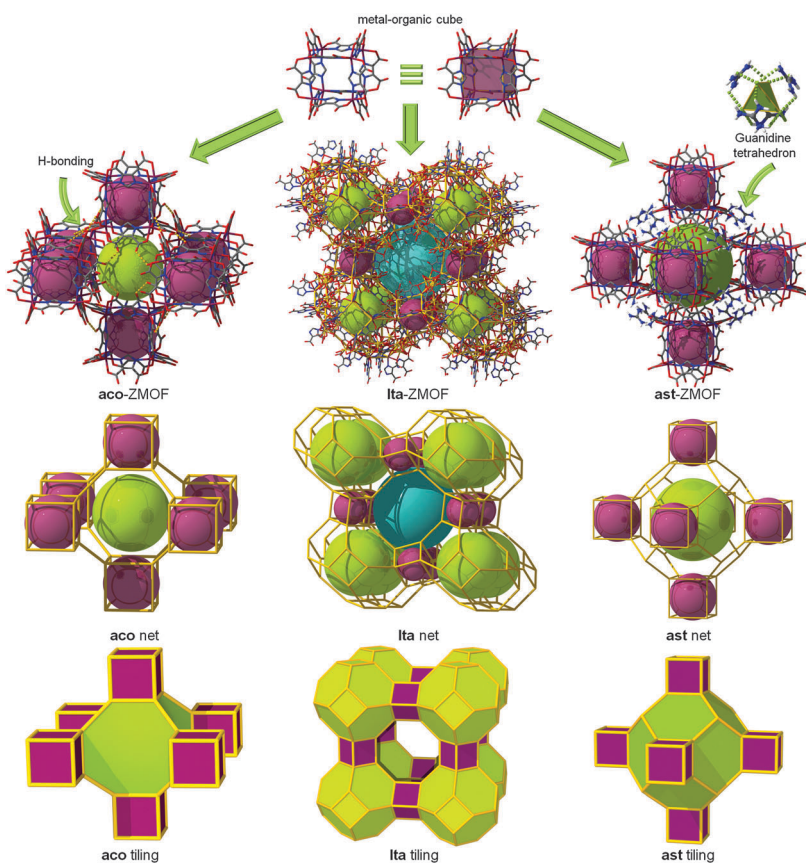
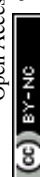


Fig. 8 MOCs can be externally functionalized to serve as SBBs for the assembly of MOFs with zeolitic topologies.



The aforementioned zeolite nets (**aco**, **ast**, **asv**, and **Ita**) are especially interesting to reticular chemistry as their nets correspond to the augmentation of the edge-transitive nets **bcu**, **flu**, **scu**, and **reo**, respectively, where the d4Rs serve as the cube-like vertex figures.<sup>53</sup> Specifically, **bcu** and **reo** are both semi-regular 8-c nets, and **scu** and **flu** are edge-transitive (4,8)-c nets.<sup>26,52</sup>

Different research groups have contributed to the development of MOC-based materials, using the vertex-linked strategy showing exclusively **pcu** or **aco** topologies.<sup>54,55</sup> Feng *et al.* also reported the reaction of Zn(II), imidazole (HIm), and 5-methylbenzimidazole (HMBIm) in the presence of (±)-2-amino-1-butanol and benzene, which yielded the zeolitic network, TIF-3, with **aco** topology based on the  $[\text{Zn}_8(\text{Im})_6(\text{MBIm})_6]^{4-}$  cluster as a cubic MOP.<sup>55</sup>

**Edge-linked MOCs.** Xu *et al.* reported  $([\text{Li}_{11}(\text{Ni}_8\text{L}_{12})(\text{H}_2\text{O})_{12}]\text{-Li}_9(\text{H}_2\text{O})_{20})_n$  in which  $[\text{Ni}_8\text{L}_{12}]^{20-}$  MOPs are bridged *via* the four oxygen atoms from two edge-ligands of two adjacent cubic MOPs. Of the twelve edges of the cubic MOP, only six edges are alternately linked to the six adjacent cubic MOPs. This MOP can be considered as an octahedral 6-c node, and hence, the network can be viewed as having a distorted **pcu** network topology (Fig. 9).<sup>54</sup> Chen *et al.* reported a MOF based on a doubly edge-center-linked cubic MOP exhibiting a **pcu** topology. Indeed, the arrangement of doubly-linked cubic MOPs, considered as a 6-c octahedral node, displays primitive cubic packing (Fig. 10).<sup>56</sup>

**2.2.3. Assembly of octahedral SBBs.** The first octahedral (**oct**) MOP, made by bridging indium metal centers with 2,5-pyridinedicarboxylates, was introduced by Eddaoudi's group in 2005.<sup>57</sup> Later the same year, a carboxylate-based MOP, MOP-28, was reported by Yaghi *et al.* in 2005, and was synthesized by the

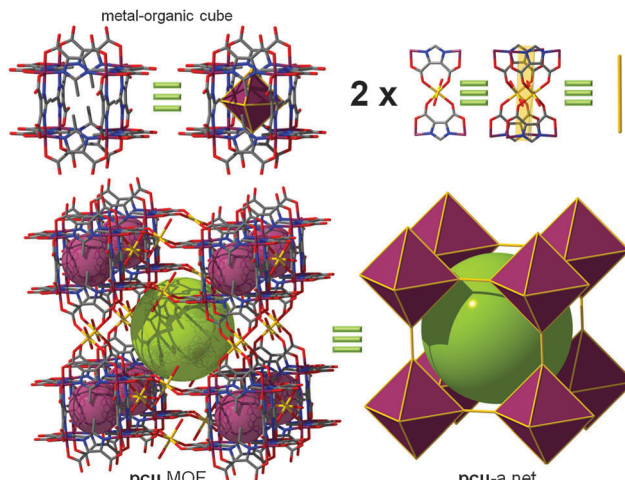


Fig. 10 Double edge-cross linkage of MOCs leads to a MOF with underlying **pcu** topology, where the MOC is 6-c, forming an octahedral SBB.

assembly of copper paddlewheels with 2,2':5',2''-terthiophene-5,5''-dicarboxylate (TTDC).<sup>36</sup> Each MOP is composed of 6  $\text{Cu}_2(-\text{O}_2\text{CR})_4$  paddlewheel building blocks and 12 *cis,cis*-terthiophene ligands. Each paddlewheel (square) has two terminal ligands: One water molecule pointing inward and one *N*-methyl-2-pyrrolidone pointing away from the center of the truncated octahedral cage.

In 2009, Zhou *et al.* reported a related MOP built up from 9*H*-carbazole-3,6-dicarboxylate (CDC). It was anticipated that the N-H functional groups of the ligands would form hydrogen bonds with appropriate solvent molecules, improving the solubility of the ensuing MOP. The  $\text{Cu}_2(-\text{O}_2\text{CR})_4$  paddlewheel clusters occupy the six corners of an octahedron, while labile terminal ligands cap the two axial positions of paddlewheel units. The ligand substitution of the outer labile axial ligands with bridging ditopic organic linkers, here 4,4'-bipyridine, leads to the formation of an extended structure from this MOP with **pcu** topology (Fig. 11).<sup>38</sup> The resulting MOF can alternatively be described as a 5-c net of **cab** topology. Specifically, the net corresponds to **cab-c** (twofold catenated **cab**) topology and contains the octahedral MOP based on CDC as a 2-c bent edge and the paddlewheel cluster  $[\text{Cu}_2(-\text{O}_2\text{CR})_4]$  as a 4-c square planar MBB. The octahedral MOP is further interconnected *via* 4,4'-bipyridine linkers to the network of a **cab** (**pcu-a**) topology based on the octahedral MOP as a 6-c octahedral SBB.

Furthermore, by using the versatility of the above described CDC-based SBB, but now bridging them through functionalization of the bent position of the ligand, this octahedral SBB can also be regarded as a 12-c cuboctahedron (the same principle as depicted in Fig. 4). This SBB is amenable to the formation of a MOF with **fcu** topology (Fig. 12).<sup>22</sup>

In fact, the first examples of SBB-based **fcu**-MOFs were published by Eddaoudi, Zaworotko, *et al.* in 2008.<sup>23</sup> The topology of the resultant MOFs (e.g.,  $[\text{Ni}_2(\text{ABTC})(\text{H}_2\text{O})_3]$  ( $\text{H}_4\text{ABTC}$  = 3,5-dicarboxyl-(3',5'-dicarboxylazophenyl)benzene)) can be rationalized in two different but equally valid ways. The octahedral building unit can be interpreted as a 12-c SBB, in which the squares are assembled by connecting the centroids of the benzene rings. A decorated cuboctahedron SBB of formula  $\text{M}_6\text{L}_{12}$

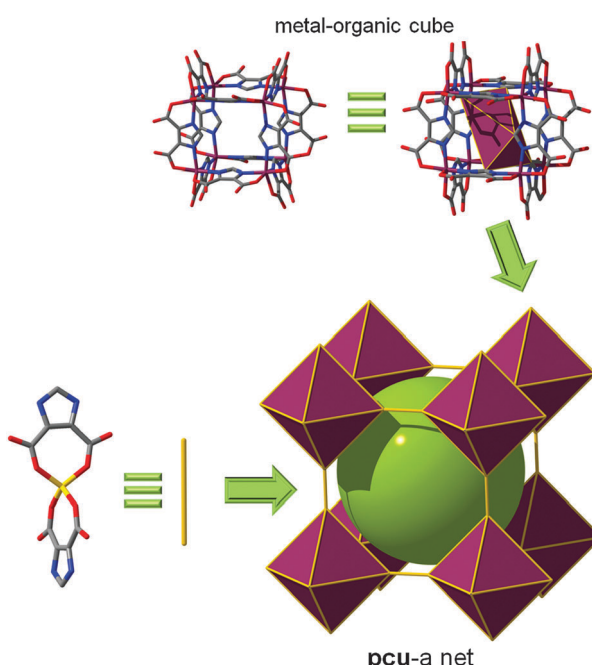


Fig. 9 Cross-linkage of Ni-based MOCs by half of their vertices with Li leads to a MOF with underlying **pcu** topology, where the MOC is 6-c, forming an octahedral SBB.



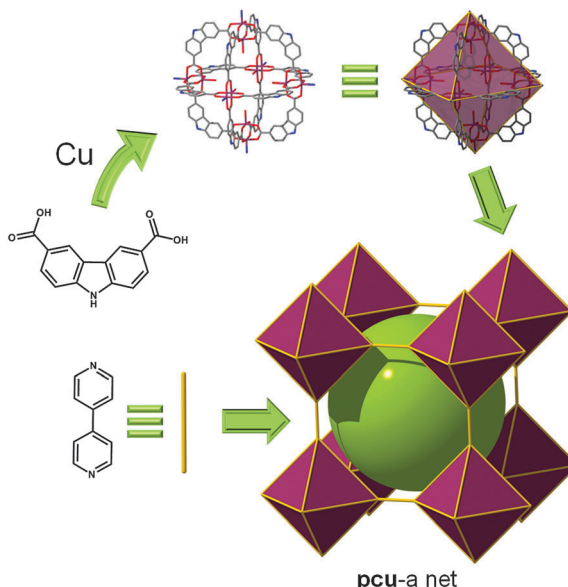


Fig. 11 Linear bridging of the CDC-based MOP through the apical position of the six paddlewheels leads to an SBB-based MOF with **pcu** topology.

is thereby revealed. The SBBs are connected through the ligand to generate the observed face-centered cubic (**fcu**) network. On the other hand, if one selects to choose the carbons of the carboxylates as a point of extension, then the framework can be interpreted as a MOF assembled from two distinct 4-c nodes: a square MBB and a rectangular ligand. The  $M_6L_{12}$  moieties would be regarded as an assembly of squares, rectangles, and hexagons, generating cages resembling those in the zeolite structure sodalite. In these MOFs, the twelve-connected SBB is not made from regular paddlewheels, as the  $120^\circ$  angle from the terminal isophthalate moieties would not allow the formation of a cuboctahedron. The SBB is then made from “pseudo-paddlewheels” constructed from two crystallographically independent metals, which adjusts for the necessary angle.<sup>23</sup>

This MOF can alternatively be described as an **nbo**-MOF, or as a (3,4)-c net of a **tfb** topology when the 4-c ligand is regarded as two 3-c nodes.<sup>58</sup> Twelve 1,3-benzenedicarboxylate (1,3-BDC; m-BDC; isophthalate) groups of the tetracarboxylate ligands and six  $M^{(II)}$  ions from an octahedral MOP as 2-c edges and 4-c corners, respectively, in the network. The MOP as an SBB was further interconnected to the twelve neighboring/surrounding MOFs in cubic close packing arrangement through the twelve edge-centers of the octahedral MOP in the (3,4)-c network of **tfb** topology.

**2.2.4. Assembly of cuboctahedral SBBs.** Yaghi *et al.* and Zaworotko *et al.* simultaneously discovered the first cuboctahedron MOP (the aforementioned MOP-1) formulated as  $Cu_{24}(1,3-BDC)_{24}(DMF)_{14}(H_2O)_{60}(DMF)_6(C_2H_5OH)_6$ .<sup>34,35</sup> The simplest way to describe the structure is to consider that each square and link of the cuboctahedron have been replaced by the paddlewheel (square MBB) and the 1,3-BDC (two-connector) units, respectively, to give an augmented cuboctahedron (truncated cuboctahedron, 4.6.8 Archimedean polyhedron).<sup>59</sup> The use of this MOP as an SBB can give rise to MOFs with different topologies depending

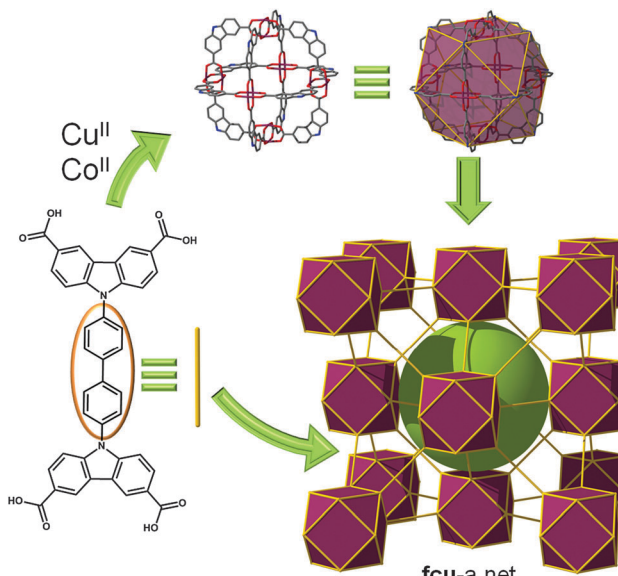


Fig. 12 Linear bridging of the CDC-based MOP by the bent position of the twelve ligands (*i.e.*, using a tetracarboxylate ligand) leads to an SBB-based MOF with **fcu** topology.

on the way the decoration occurs. Similarly to the octahedron SBB, and, as mentioned above, the points of extension can be through the vertices, by functionalizing the 5-position of the bent ligand, or through the center of square faces *via* a ligand coordinating to the apical position of the paddlewheel.

**pcu topology.** To the best of our knowledge, only the first way of decoration described previously can be applied to allow the crystallization of MOFs with **pcu** topology. Moreover, the functionalization of the 5-position of the bent ligand involves, depending on its length and flexibility, three kinds of linkage of the cuboctahedra between: (i) the same two square faces, called A-A, (ii) the same square nodes, called B-B, or (iii) between one square face and one square node, called A-B (Fig. 13).

In 2007, Zaworotko *et al.* reported a MOF built from such an SBB. A tetracarboxylate ligand was designed with the aim of employing/linking MOFs *via* the 5-position of 1,3-benzenedicarboxylate moieties. The authors noted that one cuboctahedral MOP is quadruply edge-center interlinked to the six neighboring MOFs in a primitive cubic arrangement *via* the 24 edge-centers of the MOP (Fig. 14). In other words, two different kinds of quadruple linkages, two AA-type and four BB-type are observed leading to a **pcu** underlying topology.<sup>60,61</sup> Alternatively, the structure can be deconstructed in a different way to afford **mjz** topology. In 2009, Lah *et al.* reported an isoreticular analogue using 1,3-bis(3,5-dicarboxyphenylethynyl)benzene as the ligand.<sup>62</sup>

Zhou *et al.* reported another MOF, PCN-12,<sup>63</sup> illustrating a quadruply edge-center-linked cuboctahedral MOP. However, although the net has the same **pcu** underlying topology, the types of the quadruple linkages differ from those described in the previously cited MOFs. While two different kinds of quadruple edge-center-linkages, AA-type and BB-type, are observed in the former, only one different kind of quadruple edge-center-linkage,

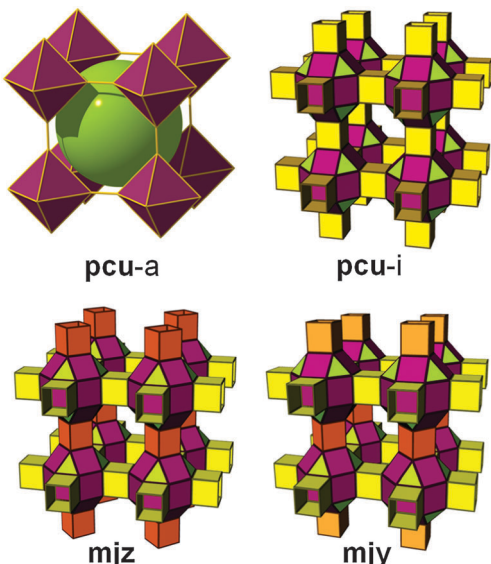


Fig. 13 Different possible ways for the quadruple cross-linking of 24-coordinated rhombicuboctahedron affording underlying **pcu** topology.

AB-type, between the square face of the cuboctahedral MOP and the square node of the cuboctahedral MOP is observed in the current MOF.

**bcu topology.** To the best of our knowledge, only one SBB-based MOF exhibiting a **bcu** topology is reported. Zaworotko *et al.* isolated the conditions to synthesize a sulfonated anionic MOP, formulated as  $[(\text{Cu}_2(5\text{-SO}_3\text{-1,3-BDC})_2(4\text{-methoxypyridine})_{0.50}(\text{MeOH})_x(\text{H}_2\text{O})_{1.50-x}]^{24-}$ , by modular self-assembly in MeOH under ambient conditions of 5-SO<sub>3</sub>-1,3-BDC moieties, Cu(II) cations, and coordinated base (4-methoxypyridine) molecules.<sup>64</sup> Importantly, all

24 sulfonate moieties are exposed at the exterior of the nanoball, which is pseudooctahedral in symmetry. They are therefore predisposed for coordination to Cu(II), and, in the presence of excess copper(II) nitrate, 16 sulfonate moieties bind to 16  $[\text{Cu}(\text{methoxypyridine})_4]^{2+}$  cations, thus facilitating cross-linking *via* axial coordination to a second sulfonate moiety in the adjacent nanoball. The cuboctahedral MOPs are doubly interconnected to the edge-centers of the eight adjacent MOPs *via* the coordination of the sulfonate group at an edge-center to a 2-c  $[\text{Cu}(\text{methoxypyridine})_4]$  node. Because of the symmetry of the MOP, the crystal packing is necessarily bcc giving rise to a **bcu** underlying topology (Fig. 15). This MOF can alternatively be described as having a **gjm** topology.

**fcu topology.** The deliberate construction of MOFs displaying a 12-c **fcu** topology using this type of cuboctahedron MOP is achievable only by functionalization of the axial position of the paddlewheel with a linear ligand due to the symmetry of the MOP. Of course, the modularity of the MOP (e.g., different metals, the large choice of ditopic bent ligands, functionalized or unfunctionalized) leads to a high number of possible combinations and hence a large number of potential MOFs.

To illustrate this strategy, we describe here the first example,  $[\text{Zn}_4(1,3\text{-BDC})_4(\text{DABC})_2(\text{OH}_2)_2]$  (DABC = 1,4-diazabicyclo[2.2.2]-octane), reported by Chun (Fig. 16).<sup>65</sup> The twelve corners of the cuboctahedral MOPs represented by the Zn(II) paddlewheel are then connected to the other neighboring cuboctahedral MOPs *via* the ditopic DABC. This structure can alternatively be described by considering the Zn(II) paddlewheel as a 5-c MBB giving rise to a **ubt** topology.

To exemplify the versatility of this SBB-based **fcu** platform, other examples have been reported, substituting Zn with Co

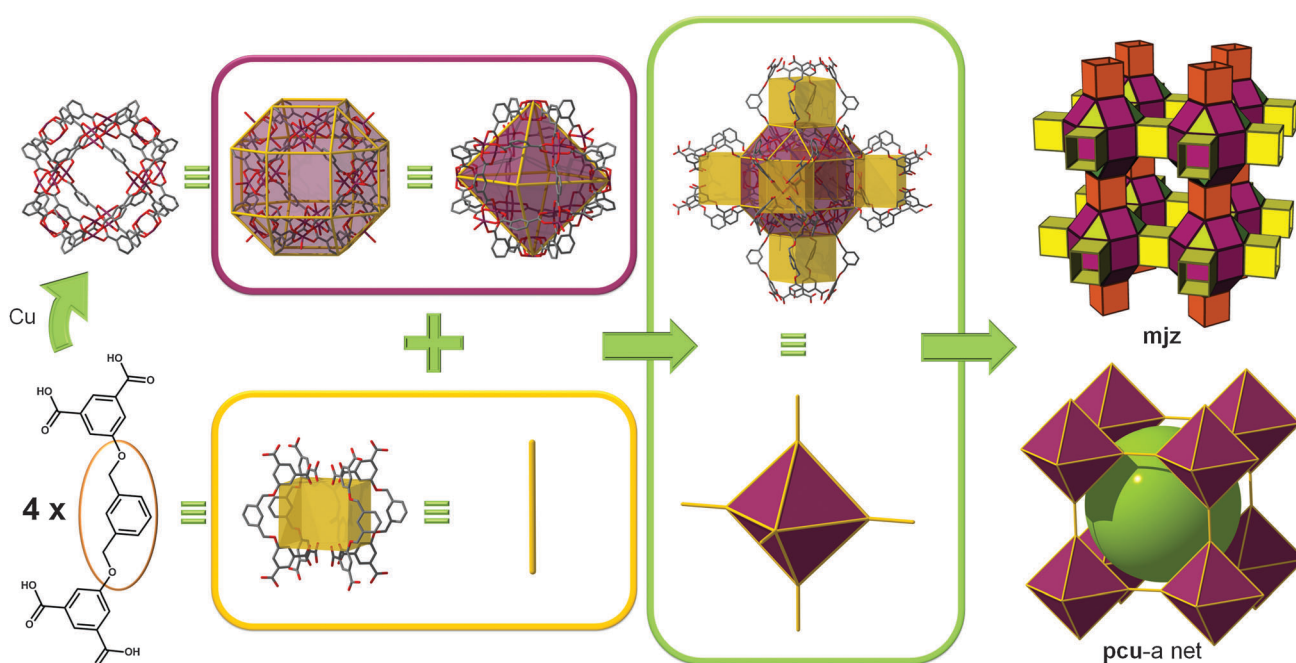


Fig. 14 Quadruple cross-linking of MOP-1 leads to an SBB-based MOF with **pcu** topology.



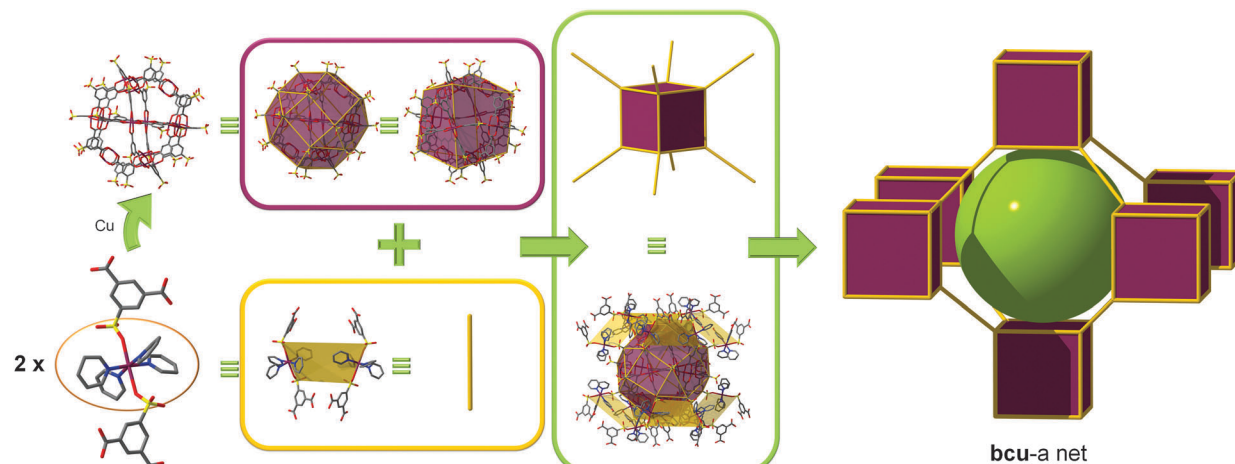


Fig. 15 Double cross-linking of functionalized MOP leads to an SBB-based MOF with **bcu** topology.

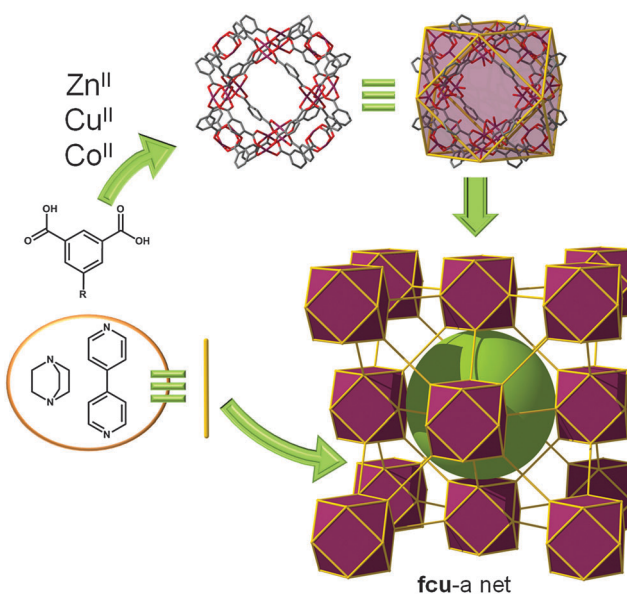


Fig. 16 Linear bridging (using DABCO or 4,4'-bipyridine) of MOP-1 analogues by the apical position of the twelve paddlewheels leads to an SBB-based MOF with **fcu** topology.

(*i.e.*, metal substitution),<sup>66</sup> replacing the *m*-BDC by 2,7-naphthalene-dicarboxylate (*i.e.*, enlargement of the 12-c SBB),<sup>66</sup> or using the amino-functionalized MOP-14 (*i.e.*, decoration of the 12-c SBB)<sup>67</sup> with bipyridine (*i.e.*, expanding the available space between the SBBs).<sup>67</sup>

**rht topology.** As depicted in Fig. 4, the cuboctahedral MOP-1 can also be regarded as a 24-connected rhombicuboctahedron SBB, where the MOP can be externally functionalized at the 5-position of the 1,3-BDC ligand, and thus afford the establishment and peripheral exposure of 24 points of extension for potentially linking the MOPs into a 3-periodic MOF. Although MOP-1 was first reported in 2001, its potential use as an SBB was not fully recognized until 2007 by Eddaoudi *et al.*

This foreseen deferred recognition is mainly due to the late enumeration of the singular (3,24)-c edge-transitive net, **rht** net, with associated vertex figures as a rhombicuboctahedron for the 24-connected vertex and a triangle for the 3-connected vertex, overlooked in the original list of enumerated 3-periodic edge-transitive nets and then recognized and appended to the list by O'Keeffe *et al.* mid-2007.<sup>68</sup> The disclosure of the **rht** net, the only (3,24)-c edge-transitive net, combined with the fact that edge-transitive nets are suitable targets in crystal chemistry immediately prompted Eddaoudi's group to explore various avenues to transpose and reveal the **rht** topology in MOF chemistry. Nevertheless, MBBs with connectivity of 24 are presently too intricate to be systematically obtained by means of simple organic ligands or polynuclear clusters. The scarcity of 24-connected MBBs, in particular, and the difficulty in isolating reaction conditions that permit the formation of highly-connected MBBs (*i.e.*,  $\geq 12$ ) have triggered the naissance of the idea and founding of the SBB approach as a means to access highly-connected (*i.e.*,  $\geq 8$ ) building blocks and subsequently use them for the construction of highly-connected MOFs.

As soon as this edge-transitive **rht** net was disclosed as a plausible net for the assembly of 3- and 24-connected building units (not as a chemical structure), Eddaoudi *et al.* pioneered and employed the SBB approach for the deliberate construction of MOFs with **rht** topology. Introduction of **rht**-MOFs was based on the employment of the functionalized cuboctahedral MOP-1 as a 24-connected rhombicuboctahedron SBB, where the MOP is externally functionalized at the 5-position of the 1,3-BDC, and a Cu-trimer as the cross-linking 3-connected MBB (Fig. 17).<sup>13</sup> Concurrently, Lah *et al.* employed a hexacarboxylate (what we term "trefoil") ligand that afforded the construction of the first disclosed **rht**-MOF based on covalently linked 3-c nodes.<sup>69</sup>

Comprehensively, the **rht** net is a singular net for the assembly of 24-c vertices (rhombicuboctahedral, **rco**) and 3-c vertices (triangular). Indeed, trigonal or 3-c organic ligands can be readily synthesized, allowing for a high degree of tunability or choice in the trigonal MBBs (Fig. 19). In contrast, 24-c MBBs are relatively rare, and organic molecules with high connectivity

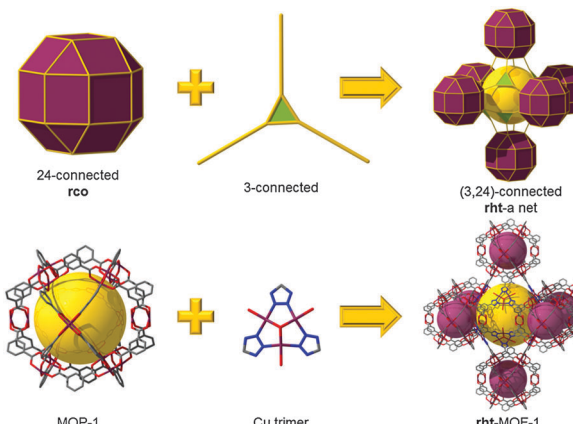


Fig. 17 Schematic depicting the design strategy for obtaining rht-MOF-1.

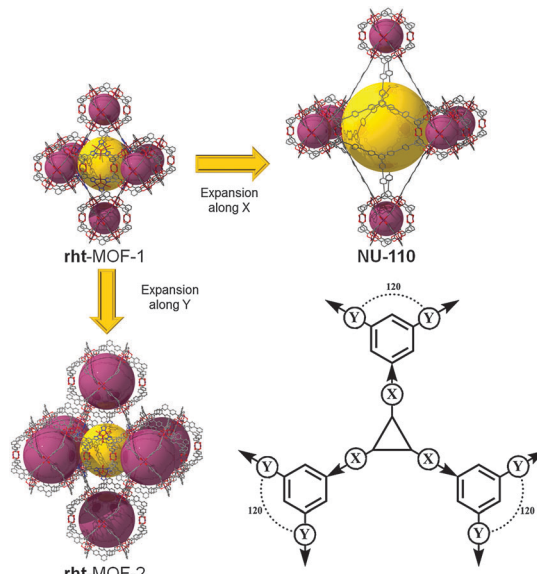


Fig. 18 rht-MOF platform tuning pathways. (X) Modification of the distance between the SBB and the central triangular core MBB. (Y) Expansion of the SBB. (Δ) Substitution of the central triangular core.

typically lack sufficient solubility required for MOF synthesis. Therefore, the SBB approach is ideal, utilizing externally (based on the bent position of the ligand) functionalized cuboctahedral MOPs as rhombicuboctahedral SBBs and thus allowing access to the requisite high-connected vertices (*i.e.*, rco) necessary for the construction rht-MOFs.

The SBB strategy was exemplified in the original report of the first rht-MOF.<sup>13</sup> By including tetrazole functionality at the 5-position of the isophthalic acid (1,3-BDC) precursor, a rhombicuboctahedron having 24 external tetrazole groups (a 24-c vertex with rhombicuboctahedral geometry) could be formed *in situ*. Under appropriate conditions, the external tetrazoles form trimers having triangular geometry, thus allowing the linking of the MOPs, resulting in the formation of rht-MOF-1.

It is worth mentioning, from a pure topological analysis perspective, that the rht-MOF-1 can be deconstructed into basic building blocks, namely 3-c and 4-c MBBs. Accordingly, as stated in the original paper, rht-MOF-1 can be alternatively described as a (3,3,4)-c net based on its basic building blocks (recently dubbed ntt). Nevertheless, such a description, based on employment of the information solely built in the 3-c and 4-c MBBs, does not provide the requisite coded information for the directed formation of rht-MOFs, *i.e.*, simple combination of three distinct basic 3-c and 4-c MBBs is not sufficient for the design of rht-MOFs. Whereas, the SBB approach permits the use of the functionalized cuboctahedral MOP-1 as a 24-connected rhombicuboctahedron SBB, the rht-coded building units (rht-cBUs), where precise embedded geometrical information codes uniquely and matchlessly for the rht net and the deliberate construction of rht-MOFs.

It has recently been demonstrated that this rht platform can be tuned *via* five basic pathways (Fig. 18):<sup>12</sup>

- (1) Expansion of the SBB
- (2) Modification of the distance between the SBB and the trigonal MBB
- (3) Substitution/modification of the triangular MBB
- (4) Functionalization of the ligand
- (5) Use of different metals (Cu, Zn, Co, *etc.*).

Thus, this patented strategy<sup>24</sup> allows the easy expansion and decoration of the SBBs on demand and also allows us to “choose”

a cationic or neutral MOF through use of the tetrazole-based trigonal MBB or use of the purely organic MBB (trefoil ligand), respectively.<sup>12</sup>

The singular nature of the rht net (*i.e.*, the sole net for the combination of 3-c and 24-c nodes) offers a high/unprecedented degree of predictability toward its successful transposition in MOF chemistry. Of additional importance, the rht-MOF platform offers independent expansion parameters (without concern for interpenetration; *i.e.*, not self-dual), which has led to one of the highest levels of tunability achieved in MOFs. This feature is clearly reflected in the large number of rht-MOF structures reported in the open literature; since the first public report in January 2008,<sup>13</sup> almost fifty derivative rht-MOFs have been reported (Fig. 19).<sup>12,13,20,21,69–85</sup> The rht-MOF platform allows access to MOFs with unprecedented surface areas; namely NU-110, based on an expanded trefoil ligand, has exhibited one of the highest BET surface areas ( $S_{\text{BET}} = 7140 \text{ m}^2 \text{ g}^{-1}$ ).<sup>86,87</sup>

**txt topology.** Up to now, the linkage between cuboctahedron MOPs can be realized in two separate ways: (i) Vertex-to-vertex, where the MOP is regarded as a 12-c SBB, or (ii) edge-to-edge fashion, where the MOP is acting as a 24-c SBB. A third possible configuration, *i.e.*, vertex-to-edge connection, is evident, which results in the cuboctahedron MOP being viewed as a 36-c SBB.

Indeed, Zhang *et al.* reported a txt-MOF with txt topology based on the (3,36)-c net. A 1,3-bis(3,5-dicarboxyphenylethynyl)-pyridine ligand was employed as a 3-c node (Fig. 20).<sup>88</sup> The cuboctahedral MOP is connected *via* the 24 edge-centers and the 12 corners (apical position of the copper paddlewheel cluster) of the MOP to six adjacent MOPs in primitive cubic arrangement *via* quadruple edge-center linkages. An amide-functionalized analogue (PCN-124) was recently found to show improved  $\text{CO}_2$  uptake at 273 K.<sup>89</sup> The network is alternatively described



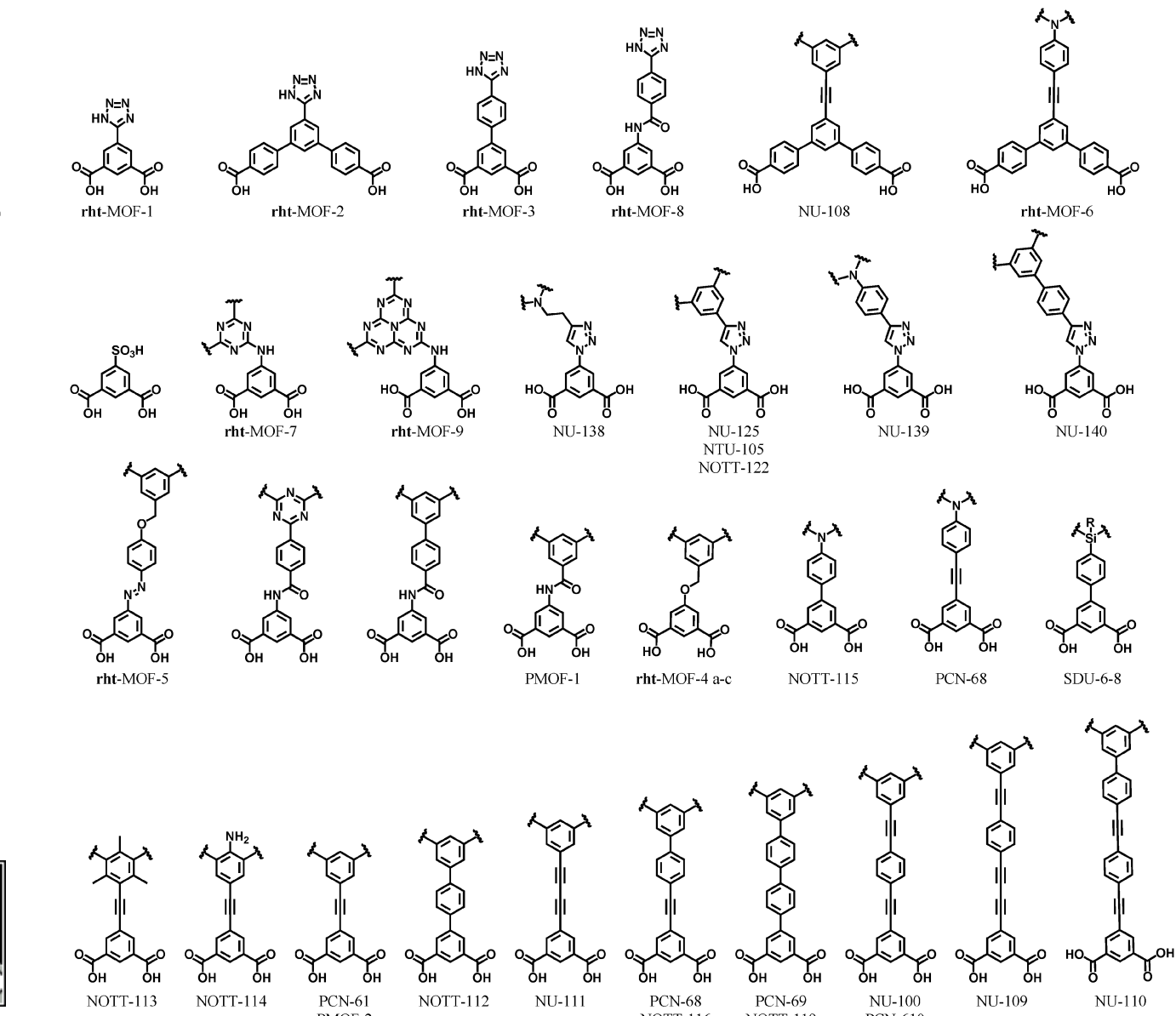


Fig. 19 Tetrazole and trefoil ligands utilized for rht-MOF synthesis. Given name(s) for the related MOF are listed, when applicable.

as a (3,5)-c net with a **pzh** topology, where the ligand was considered as a (3,3)-c node consisting of two different kinds of 3-c nodes and the  $[\text{Cu}_2(-\text{O}_2\text{CR})_4(\text{pyridyl})]$  cluster as a 5-c node.

**Other topologies.** Lian *et al.* also reported a 3-periodic network,  $[\text{Cu}_{24}(-\text{NR}_x)_4(1,3,5\text{-BTC})_{12}(\text{DABCO})_9(\text{H}_2\text{O})_6] \cdot 8(\text{NO}_3)_9$ ,<sup>90</sup> containing a cuboctahedral MOP as a 36-c SBB (Fig. 21). The network contains the characteristics of the nets of **fcu** and of **ubt** simultaneously. A 1,3-BDC unit of the 1,3,5-BTC ligand acts as an edge and the  $[\text{Cu}_2(-\text{O}_2\text{CR})_4]$  paddlewheel cluster as a 4-c MBB, forming cuboctahedral MOP as an SBB. The 4-c  $[\text{Cu}_2(-\text{O}_2\text{CR})_4]$  paddlewheel clusters of the cuboctahedral MOP are interconnected to twelve other cuboctahedral MOPs in a cubic close packing arrangement *via* DABCO linkers, as in the network of the **fcu** topology, and the three adjacent cuboctahedral MOPs in the

network are further interconnected *via* a 3-c  $[\text{Cu}_3(-\text{NR}_x)(-\text{O}_2\text{CR})_3]$  cluster, as in the network of the **rht** topology. In addition, the eight  $[\text{Cu}_3(-\text{NR}_x)(-\text{O}_2\text{CR})_3]$  clusters at the corners of a cube are further interlinked *via* DABCO linkers to a cubic cage at the octahedral cavity of the cubic close packing arrangement of the cuboctahedral MOPs leading to a (3,5,6)-c net of **ott** topology (Fig. 21).

**Comparison of ntt, ubt, nut, and ott topologies.** All the nets of **ntt**, **ubt**, **nut**, and **ott** topologies are based on the same cuboctahedra, as an SBB, in cubic close packing arrangement (Fig. 22). In the (3,4)-c net of **ntt** topology, three cuboctahedra in close contact are interconnected *via* 3-c node through the edge-centers of the cuboctahedron (Fig. 22a). Whereas the three cuboctahedra in the 5-c net of **ubt** topology are interconnected

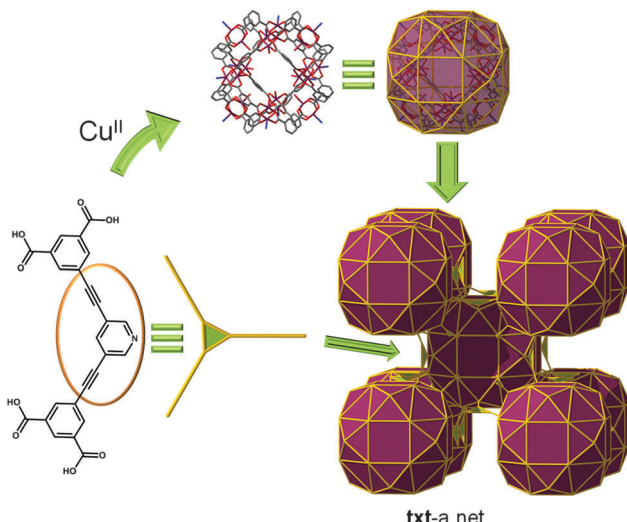


Fig. 20 Connection of MOP-1 by the bent position of the twenty-four ligands (isophthalate ends) and apical position of the twelve paddlewheels (pyridine end) leads to an SBB-based MOF with **txt** topology.

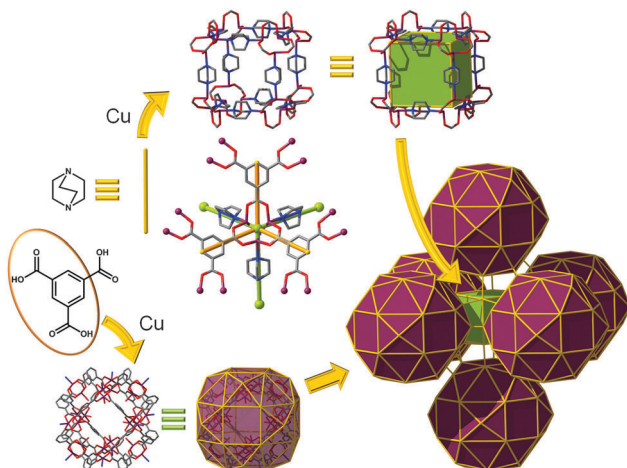


Fig. 21 **ott**-type MOF: The cuboctahedral MOPs are 36-connected. The 24 BTC ligands are linked to Cu-trimmers  $[\text{Cu}_3(-\text{NR}_x)(-\text{O}_2\text{CR})_3]$ . Additionally, each MOP is directly connected to 12 others by bridging DABCO ligands. The  $[\text{Cu}_3(-\text{NR}_x)(-\text{O}_2\text{CR})_3]$  cluster is further linked to the other three  $[\text{Cu}_3(-\text{NR}_x)(-\text{O}_2\text{CR})_3]$  clusters by DABCO linkers, leading to a cubic cage.

via 2-c nodes through the corners of the cuboctahedron (Fig. 22b), in the (3,5)-c net of **nut** topology, the three cuboctahedra are interconnected *via* both 3-c node through the edge-centers of the cuboctahedron and 2-c node through the corners of the cuboctahedron (Fig. 22c). The networks with (3,5)-c **nut** topology are yet to be found synthetically. In the (3,5,6)-c net of an **ott** topology, in addition to the aforementioned linkages between the cuboctahedra in the net of the **nut** topology, the eight 3-c nodes, in a primitive cubic arrangement at the octahedral cavity of the cubic close packing arrangement of the cuboctahedra, are further interconnected *via* 2-c node (Fig. 22d).

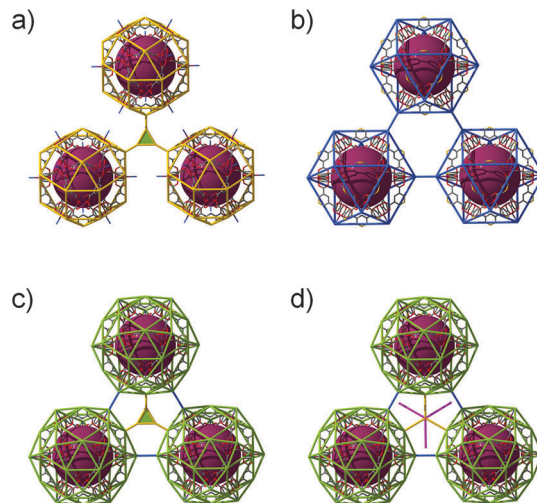


Fig. 22 (a) Three adjacent cuboctahedra in a net of **ntt** topology are linked by a 3-c node through the 24 edge-centers of the MOP. (b) Three adjacent cuboctahedra in a net of **ubt** topology are linked by a 2-c node through the 12 corners of the MOP. (c) The cuboctahedra in a net of **nut** topology are linked both by a 3-c node and a 2-c node. (d) In the net of **ott** topology, the 3-c nodes in the net of **nut** topology are further linked to the other 3-c nodes by 2-c linkers.

**2.2.5. Assembly of rhombic dodecahedral SBBs.** All the SBBs described thus far, which serve to build up MOFs, belong to the regular or quasi-regular polyhedra family. The specificity of these MOPs is that their elaboration necessitates use of one kind of link and one kind of vertex contrary to the rhombic dodecahedron (**rdo**), which is composed of two different vertices, *i.e.*, 3-c and 4-c. If the cuboctahedral cage constructed solely from 4-c paddlewheels (MOP-1 and related) is considered as an “alpha” cage, this **rdo** cage can be considered as its “beta” equivalent, which is logical, as the **rdo** polyhedron is the dual of the **cuo** polyhedron, therefore, the middle of their edges both match with the vertices of a rhombicuboctahedron.

**pcu topology.** Lah *et al.*<sup>91</sup> reported the use of a 3-c organic node and a 4-c node leading to a (3,4)-c rhombic dodecahedral MOP. When the 4-c node of the MOP is further linked *via* an additional 2-c linker, the network based on a corner-linked rhombic dodecahedral MOP as an SBB could be achieved (Fig. 23). In this case, the rhombic dodecahedral MOP is considered as a 6-c SBB (octahedron) giving rise to a net of **pcu** underlying topology.

Zhang *et al.*<sup>92</sup> reported a rhombic dodecahedral (**rdo**) based SBB built using six  $[\text{Zn}_2(-\text{O}_2\text{CR})_4]$  clusters as 4-c MBBs, eight  $[\text{Zn}_2(-\text{O}_2\text{CR})_3]$  (or  $\text{Zn}(-\text{O}_2\text{CR})_3$ ) clusters as 3-c MBBs and the 1,3-BDC groups as the 24 edges. Each of the rhombic dodecahedral MOPs are quadruply interconnected between two square nodes of six neighboring MOPs in a primitive cubic packing arrangement giving rise to a **pcu** underlying topology. However, the rhombic dodecahedral MOP can alternatively be regarded a (3,4)-c net having **zjz** topology (Fig. 24).

**rht topology.** Recently, Sun *et al.* reported a very interesting zinc hexacarboxylate, containing both 3-c and 4-c paddlewheels.<sup>93</sup>



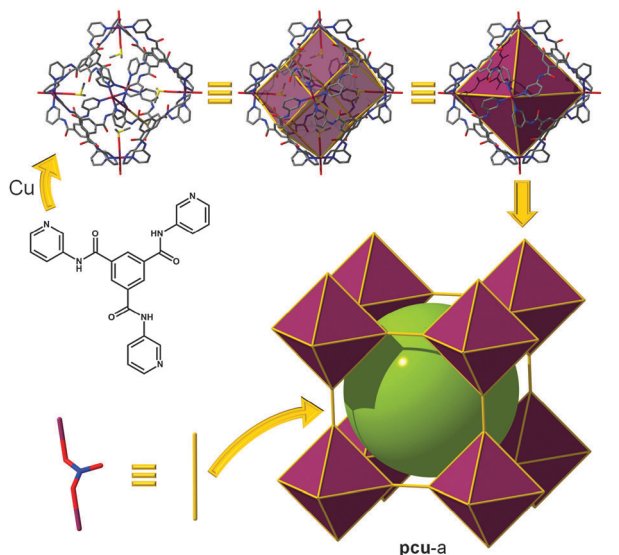


Fig. 23 Linking rhombic dodecahedral MOPs by nitrate anions leads to an SBB-based MOF with **pcu** topology.

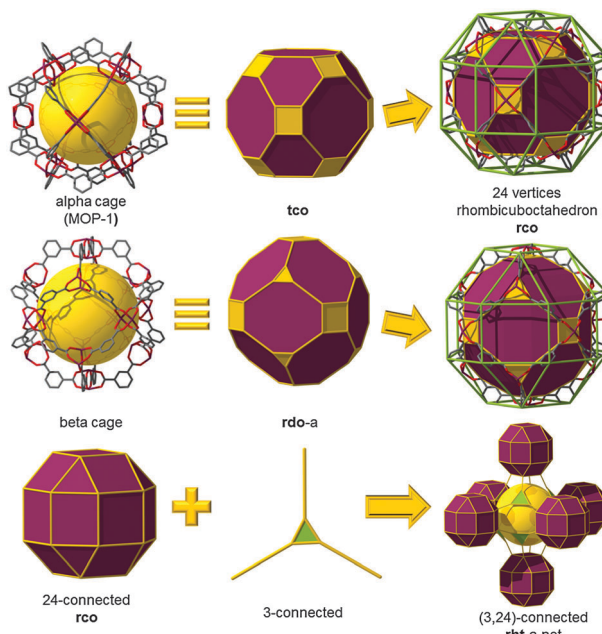


Fig. 25 Comparison of the alpha cage (**rco**) and beta cage (**rdo-a**). Considering the bent position of the ligand as vertices, both alpha and beta cages can be seen as a rhombicuboctahedron (**rco**) with 24 vertices. The only way to link **rco** with triangles leads to the edge-transitive **rht** net (represented as augmented).

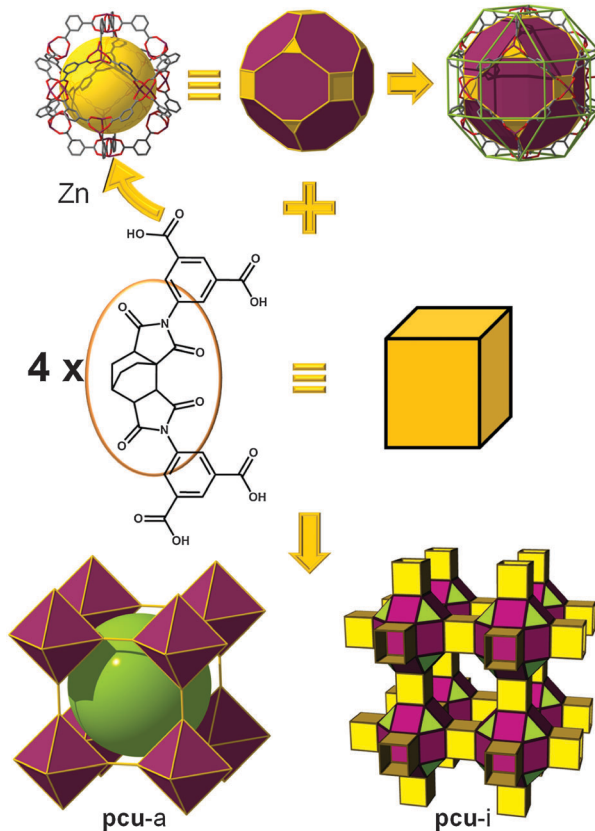


Fig. 24 Quadruple crosslinking of **rdo** SBB (points of extension defining a rhombicuboctahedron) leads to an SBB-based MOF with **pcu** topology.

As in the previous example, the structure contains the rhombic dodecahedral (**rdo**) cage built from six 4-c paddlewheels and eight 3-c paddlewheels, bridged by 24 isophthalate moieties from a trefoil-like ligand. These 24 isophthalates are cross-linked

through the central ring of the ligand in a similar fashion as the **rht**-MOFs described earlier in this review. This arrangement leads to a “beta” version of the ubiquitous (3,24)-c **rht**-MOFs (Fig. 25). The structure of this beta-**rht**-MOF can be alternatively described as a (3,3,4)-c net with **tfe** topology.

Interestingly, Yuan *et al.* simultaneously reported a zinc-trimesate, where the trigonal MBB is now substituted by another 3-c paddlewheel.<sup>94</sup> Of course, there is no doubt this type of structure (beta-**rht**-MOFs) can be expanded by increasing the size of the branches between the 3-c central core (organic or 3-c paddlewheel) and the **rdo** cage, similar to what Eddaoudi *et al.* reported for the classical “alpha” **rht**-MOFs.<sup>12</sup> Interestingly, the occurrence of the first beta-**rht**-MOF can be retroactively traced back to 2001 for a (3,3,4)-c structure reported by Zaworotko *et al.*<sup>95</sup> It is not surprising that the beta-**rht**-MOF was not recognized back then, as the SBB approach to describe and construct MOFs, a more elaborate tool permitting to recognize **net**-cBUS, was not introduced until years later in 2007.<sup>13,23,24</sup>

## 2.2.6. Assembly of tri-capped trigonal prism SBBs

**gea** topology. Finally, one of the latest additions to those highly-connected nets that are amenable to the SBB approach has been introduced recently by the Eddaoudi group, starting from the discovery of a novel (3,18)-c net, now in the RCSR and referred to as **gea** (Fig. 26).<sup>10</sup> The initial MOF, **gea**-MOF-1, revealed the discovery of a nonanuclear rare earth cluster acting as an 18-c MBB linked by triangular tricarboxylate ligands. Immediately, upon the discovery of this new MOF system, Eddaoudi’s group recognized the potential of this highly-connected net to be employed as a blueprint for the practice

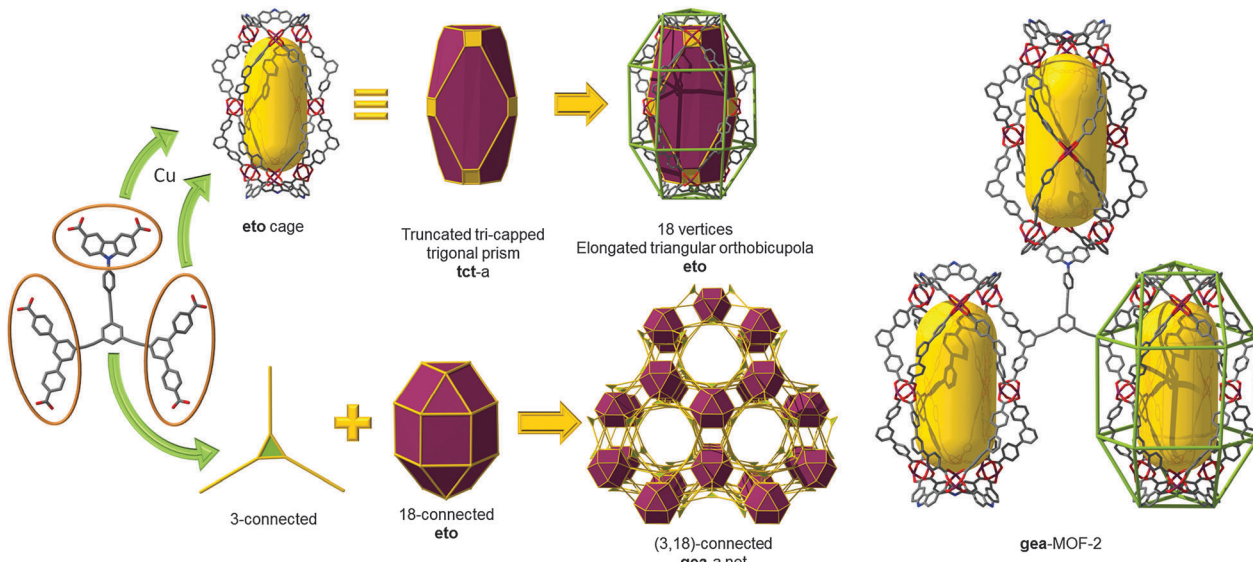


Fig. 26 Schematic showing the design path followed to achieve the construction of **gea**-MOF-2, the first SBB-based **gea**-MOF.

of the SBB approach. The requisite MOP ( $M_9L_{18}$ ), containing the coded information suitable to transpose the observed connectivity of the inorganic cluster in the parent **gea**-MOF-1, has been previously reported.<sup>40</sup> The aforementioned MOP results from the assembly of two types of bent ligands ( $6 \times 90^\circ$  and  $12 \times 120^\circ$  angles) with copper paddlewheels. After careful geometrical analysis, a trefoil-like hexacarboxylate ligand, similar to those utilized for **rht**-MOFs, was designed to include one of the predisposed dicarboxylate moieties at a  $90^\circ$  angle, and the remaining two at  $120^\circ$ . As expected, the synthesized ligand, in combination with copper (paddlewheels), resulted in the formation of the MOP-based SBB *in situ*, which are also cross-linked to form the pre-targeted **gea**-MOF-2, the first SBB-based **gea**-MOF.

It is to be mentioned that the topology of **gea**-MOF-2 can be described as a (3,3,3,4,4)-c net having **gwe** topology. Nevertheless, such a penta-nodal net is far too complicated to allow for intuitive design of this material, a **gwe**-MOF, from simple combination of five distinct basic 3-c and 4-c MBBs.

### 2.3. MOPs for MOFs: Conclusion

As elucidated through all the aforementioned examples, the SBB approach relies on the use of a MOP as an elaborate building entity, programmed in order to contain the coded information essential to construct a targeted MOF with a given topology. The MOP encloses the requisite geometrical information with desired peripheral points of extension (connectivity) that match the **net**-cBUs' coding for a selected targeted net.

The key perquisites to use the SBB approach for the design of a MOF are: (1) A blueprint net with minimal edge-transitivity, preferably singular, that is exclusive for the assembly of given building units, and not susceptible to self-interpenetration upon net expansion and/or decoration and (2) reaction conditions that permit us to consistently form the desired SBB.

## 3. Supermolecular building layers (SBLs)

Many existing 3-periodic MOFs can be interpreted as consisting of inter-connected (*e.g.*, pillared) layers (*i.e.*, 2-periodic sheets). The underlying layers can be isolated through deconstruction of the crystal structure, and *in fine*, designed and constructed from judiciously selected metals and ligands. As mentioned earlier in this review, edge-transitive nets are ideal targets in crystal chemistry. To apply this to pillared-layer structures, it is important to recognize that there are only five edge-transitive 2-periodic nets that exist, **sql** (square lattice), **kgm** (Kagomé), **hcb** (honeycomb), **kgd** (Kagomé dual), and **hex** (hexagonal lattice). Targeting these nets and their corresponding pillared versions can facilitate rational design of MOFs (Fig. 27).

Moreover, when regarded as augmented layers, it appears that, out of these five edge-transitive layered nets, two of them, **sql** and **kgm**, can be regarded as the assembly of squares (*i.e.*, they are solely composed of 4-c vertices). These nets are thus suitable to target with metals able to form the ubiquitous (and aforementioned) 4-c paddlewheel (Cu, Ni, Fe, Zn, Co, *etc.*).<sup>31,96</sup>

Hundreds of examples of pillared MOFs can be found in the Cambridge Structural Database (CSD),<sup>97</sup> most of them being quite simple pillaring, as will be described below. However, in 2011, Eddaoudi *et al.* introduced a powerful concept/strategy, namely supermolecular building layers (SBLs), that allowed the design and discovery of pillared MOFs with a much higher degree of complexity.<sup>98</sup> Of course, this unique strategy is not restricted to complex pillaring, and is also applicable to simple pillaring.

The SBL approach leverages the possibility to utilize the readily targeted 2-periodic MOF layers (SBLs) as building blocks to construct, functional 3-periodic porous MOFs. This is accomplished by chemically cross-linking the layers through accessible bridging sites on the layers (*e.g.*, open-metal site or



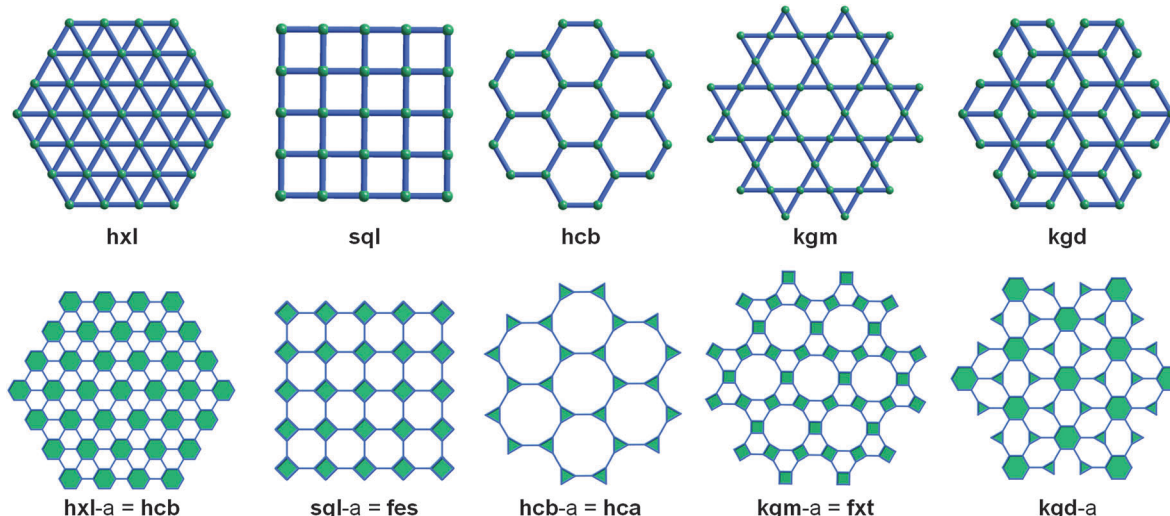


Fig. 27 Schematic of the five edge-transitive layers (top) and their augmented forms (bottom).

functionalizable position of the organic linker). This design method requires judicious selection of organic ligands that will pillar the layers. As a result of the countless cross-linking combinations, myriad MOFs having specific underlying 3-periodic network topologies can be designed and synthesized utilizing the pre-targeted SBLs. An additional advantage of this approach is the fact that the overall framework and network topology will remain constant, based on the pillared layers, allowing practically endless expansion of the confined space (*e.g.*, cavities, porosity). It can also be noted that, if the pores or windows of the layers remain unexpanded (*i.e.*, expansion of the pillar only), any concern for interpenetration, a plague of many expanded MOFs, is precluded. The inherent modularity of this method allows for facile functionalization or introduction of additional functionalities (*e.g.*, free carboxylic acid groups<sup>98</sup>) to target specific applications (*e.g.*, MOF platforms for CO<sub>2</sub> capture, gas separation, controlled drug release, *etc.*)<sup>99</sup>.

### 3.1. Axial-to-axial pillarng

The first, and apparently, most obvious way for the pillarng of MOF layers takes advantage of neighboring accessible metal sites; this can be referred to as axial-to-axial (A-A) pillarng. Perhaps the most common, readily constructed, and well-known examples involve MOFs having **sql** or **kgm** topology and are based on the aforementioned square paddlewheel dimer MBBs [M<sub>2</sub>(O<sub>2</sub>CR)<sub>4</sub>(A)<sub>2</sub>; M = metal, A = axial ligand] bridged by ditopic organic ligands [*e.g.*, benzenedicarboxylates, such as terephthalate or isophthalate]<sup>31,96,100</sup>. In these examples, the axial sites of the square (4-c) paddlewheel orient outward toward the upper and lower surfaces of the MOF layer. In 2-periodic materials, these sites are typically occupied by terminal ligands (*e.g.*, water, pyridine, or DMF) that do not play a role in the network topology. Thus, utilizing a linear, bifunctional or ditopic ligand (*e.g.*, azolated ligands, such as DABCO<sup>101–128</sup> or bipyridine<sup>113,126,129–141</sup>) allows coordination to neighboring open-metal/axial sites (*i.e.*, now 6-c, octahedral) and resultant cross-linking of separate/independent layers (Fig. 28). Thus, the

**sql**-MOFs could be employed as SBLs amenable to pillarng *via* cross-linking through linear organic linkers to construct the desired MOF platform having **pcu** topology, **pcu**-MOF, based on linear bridging of 6-c (octahedral) nodes. Surprisingly, the first and intended formation of such a MOF by Seki, Mori, *et al.* in 2001, has been barely cited,<sup>101</sup> despite a large series of isoreticular mixed-ligand **pcu**-MOFs that have since been produced, derived from their pioneering approach.

Indeed, there are many distinct examples of such **pcu**-MOFs, due to the exceptional tunability of this platform. It is possible to substitute the original Cu<sup>103,108,110,125,129,131,137,140</sup> from the SBL with other metals, such as Zn,<sup>102,104–106,108,110–119,122–126,130,132,133,135,136,138,142–157</sup> Ni,<sup>109,127,139</sup> Co,<sup>107,120,121,134,139,141,158,159</sup> Mn,<sup>160</sup> Fe,<sup>128</sup> Cu/Zn,<sup>125</sup> *etc.*, but also to vary the length (1,4-BDC,<sup>105,107,109,110,113,118,121–126,128,132,135,142,143,145–149,160</sup> 2,6-NDC,<sup>103–111,113,119,120</sup> 4,4-BPDC,<sup>135</sup> *etc.*<sup>135</sup>) or functionality (–NH<sub>2</sub>,<sup>111,114,119,160</sup> –NO<sub>2</sub>,<sup>106</sup> –F,<sup>103,113,146</sup> –Me,<sup>113,134</sup> –Cl,<sup>116,119</sup> –Br,<sup>116,119</sup> –COOH,<sup>114,129,130,137</sup> –OH,<sup>111,117</sup> –naphthalene,<sup>108,113,144</sup> –anthracene,<sup>112,115,138</sup> *etc.*<sup>102,104,136</sup>) of the dicarboxylate ligand, as well as the pillars (*e.g.*, DABCO,<sup>102–128</sup> bipyridine,<sup>113,126,129–141</sup> benzene-bipyridine,<sup>146</sup> functionalized bipyridines,<sup>143,152,154</sup> di-triazole,<sup>148</sup> *etc.*,<sup>131,133,135,140,142,144–147,149–151,153,155–157,159,160</sup> Fig. 28).

In addition to the paddlewheel-based SBL, the SBLs can be constructed from a variety of metal clusters and/or single-metal ions and organic bridging ligands,<sup>161</sup> and the pillar can be any other ditopic entity, such as organic dicarboxylates<sup>162</sup> or inorganic (*e.g.*, SiF<sub>6</sub>)<sup>163</sup> resulting in limitless possibilities for novel 3-periodic MOFs.

Another type of **sql** layered material, mainly explored by Hupp *et al.*<sup>164–175</sup> and Choe *et al.*,<sup>176–180</sup> can be constructed from 4-c carboxylate ligands, such as porphyrin tetra-benzoates, leading, in most cases, to MOFs with a (4,6)-c **fsc** topology. They can be seen as variations of the above described **pcu**-MOFs, where half of the pillars are missing, offering therefore more potential accessible voids. Interestingly, the simultaneous pillarng of paddlewheels and porphyrins can sometimes occur, leading to MOFs with **pcu** topology, but also more complex nets that we

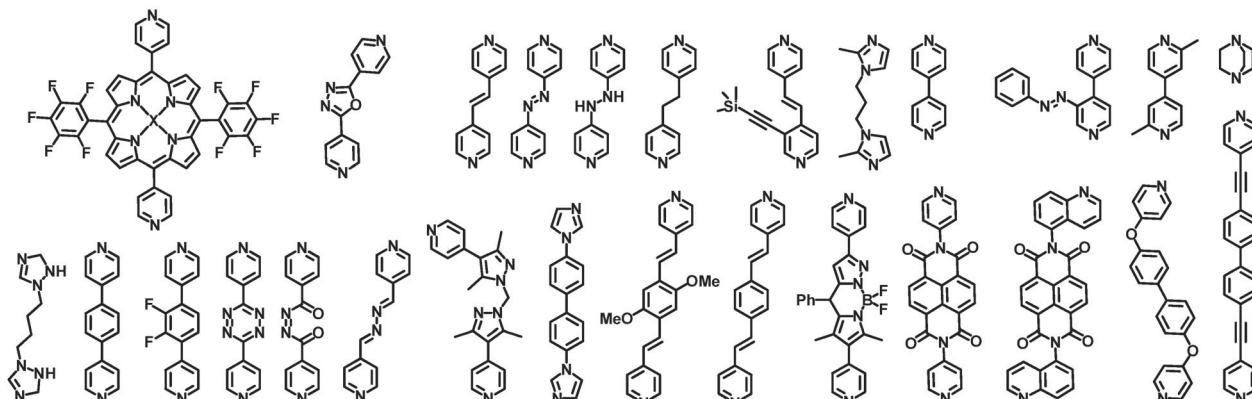
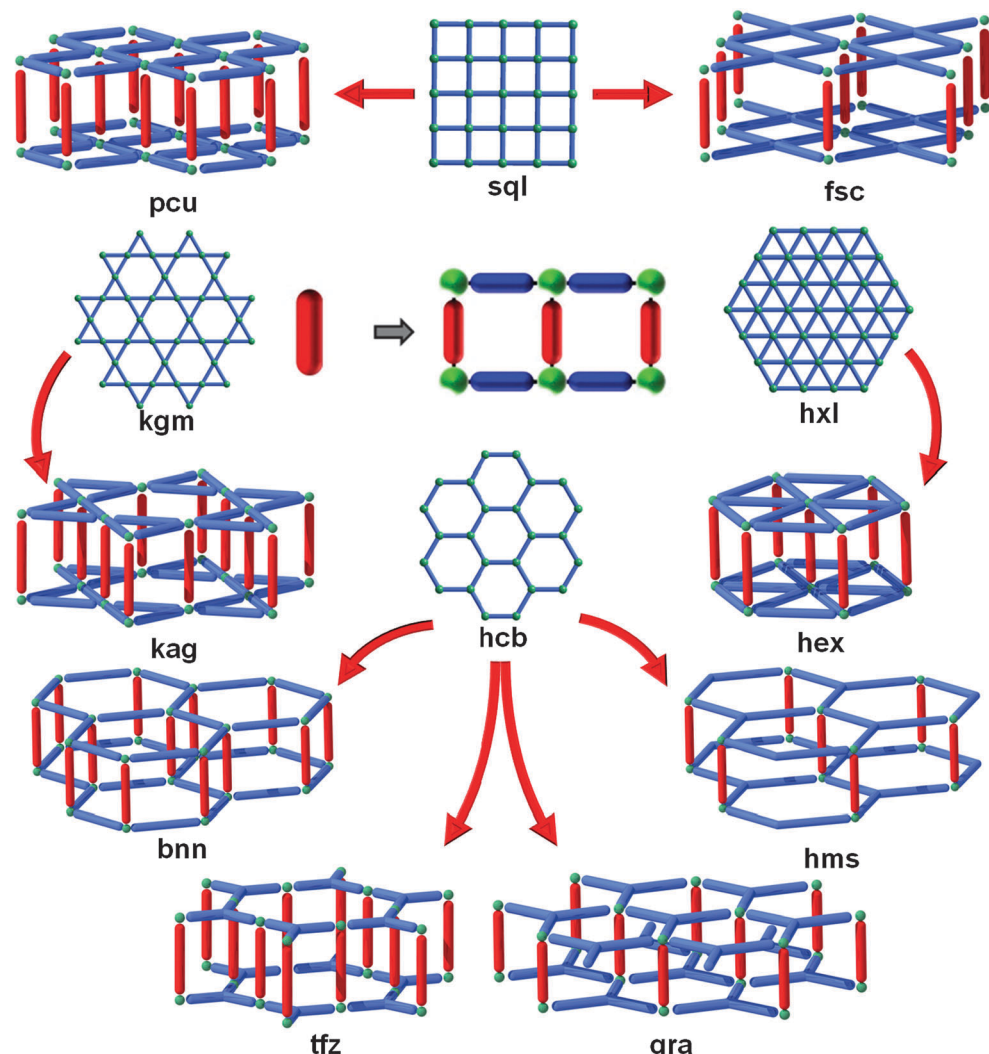


Fig. 28 Schematic of the A-A pillarating of **sql**, **kgm**, **hxl**, and **hcb** layers to form the **pcu**, **fsc**, **kag**, **hex**, **bnn**, **hms**, **gra**, and **tfz** nets (top), and a non-exhaustive list of ligands that have been used for this type of pillarating (bottom).

will not describe here, as they are not reasonably targetable as part of the SBL design strategy.<sup>176–180</sup> The first **fsc**-MOF was reported in 2007 by Feng *et al.*, based on Cu<sub>6</sub>I<sub>6</sub> and Cu<sub>8</sub>I<sub>8</sub> MBBs bridged by DABCO, but again, would be difficult to employ in a pillarating strategy.<sup>181</sup>

Interestingly, the number of **kag**-MOFs, *i.e.*, **kgm** layers pillared in the same A-A fashion is scarce. These MOFs would potentially offer more void space than their **pcu** analogues.<sup>109,123,126</sup>

Other two-dimensional layers are well-known in coordination chemistry<sup>182–184</sup> and in 2003, another example of A-A pillarating

was reported by Rosseinsky *et al.* based on  $\text{Ni}_3\text{BTC}_2$  honeycomb layers, pillared by 4,4'-bipyridine, leading to a (3,4)-c **tfz**-MOF.<sup>185</sup> Interestingly, in this SBL, Ni plays the role of a 2-c node that bridges the 3-c BTC ligands; also, it is possible to “inverse” the roles and find in the literature a layer constructed of 3-c Zn paddlewheels bridged by triptycene-dicarboxylate.<sup>162</sup> In this particular case, the ligands also act as pillars to form a 5-c net with **bnn** topology. These pillars are connected in a monodentate coordination fashion, and one can reasonably imagine replacing them by other types of ligands without affecting the formation of the SBL, as exemplified by the occurrence of related 2-periodic SBLs in the open literature.<sup>186</sup>

A variant of the **bnn** net can be achieved using Ni and trimesic acid (*i.e.*, an **hcb** SBL where both the ligand and Ni play the role of 3-c nodes), pillared by ligands such as 4,4'-bipyridine, as reported by Sun *et al.* in 2007.<sup>187</sup> In this specific case, the N-based ligand pillars the Ni, the other 3-c nodes from the layer (trimesate) remain unchanged. The resulting **hms**-MOF is then regarded as a variant of a **bnn**-MOF, with half of the pillars missing. Interestingly, Lah *et al.* reported in 2013 an interesting post-synthetic pillar exchange with DABCO, leading to fully exchanged pillars, or SBLs alternatively pillared by 4,4'-bipyridine and DABCO.<sup>188</sup> The same group gave even further contribution as they also reported a fourth type of **hcb** pillaring (**gra**), where the SBLs are staggered from one another (*versus* eclipsed in **hms**).<sup>189</sup>

By choosing the **hxl** layer as a starting point for a pillaring strategy, it is evident to target 6-c **hex**-MOFs. Despite the fact that this kind of SBL<sup>190</sup> or corresponding pillared MOFs seem difficult to produce, Vittal *et al.* reported such a **hex**-MOF in 2012.<sup>150</sup>

Finally, to the best of our knowledge, there is no reported example of pillared **kgd** SBLs. This is surely related to the unique nature of the **kgd** layer, which requires two types of nodes for its formation (3-c and 6-c nodes), making it extremely challenging to target. If such a 2-periodic MOF is achieved, it will not necessarily be compatible with the SBL approach (*i.e.*, may not be “pillar-able”).<sup>190</sup>

### 3.2. Ligand-to-ligand pillaring: **ssa**-MOF, **ssb**-MOF, **lvt**-MOF, **pts**-MOF, **lon**-MOF, and **nbo**-MOF platforms

Another SBL cross-linking/pillaring method involves multifunctional ligands for linear pillaring, though perhaps in a less obvious manner. In the case of the square paddlewheel based SBLs, there are positions on the organic bridge (*e.g.*, 5-position on isophthalate) that orient outward toward the upper and lower surfaces of the MOF layer. These sites are readily modified through conventional organic chemistry. Through appropriate design of the ligand, these positions from two neighboring layers can be chemically bridged, thus covalently pillaring the layers. In other words, specific ligands are selected/designed to simultaneously contain two bridging ligand moieties (*e.g.*, di-isophthalate, “X”- or “T”-shaped) that pillar adjacent layers through the covalent linkage within the tetracarboxylate ligand (Fig. 30). This method of cross-linking SBLs, so called ligand-to-ligand (L-L) pillaring, where the 4-c ligand coordinates to form the 4-c paddlewheel MBB, results in 3-periodic MOFs based on an underlying (4,4)-c topology.

We mentioned earlier in this review that the assembly of 4-c paddlewheels with 2-c ligands, such as isophthalates, can lead to two types of edge-transitive layers, **sql** or **kgm**. However, a close examination of the structures from the CSD,<sup>97</sup> will reveal that it is possible to distinguish at least two types of **sql** layers, where the arrangement of the isophthalates around the paddlewheels differs. Taking into account the fact that the isophthalate ligand is bent, this will lead to several distinct L-L pillaring possibilities, as the functionalized position (5-position of isophthalate) of the ligand will alternately point up or down from the **sql** layer, but in a different fashion, as depicted in Fig. 29. This statement is generally applicable to **sql** layers built from paddlewheels and various ligands including isophthalate-based moieties.

A third variation can occur in the event that the 4-c node is of tetrahedral geometry. An example is by reacting salts of 6- to 8-coordinate metals (*e.g.*, indium) and isophthalate-based ligands.<sup>191</sup> In this manner, it is possible to target a third type of **sql** layer, **sql-3**, where the bent position of the isophthalates is alternately pointing up and down. Even though this **sql-3** layer is probably more difficult to achieve compared to the ones based on paddlewheels, it allows *in fine* some additional interesting pillaring possibilities, as will be described later in this review.

This L-L pillaring type can be divided into two distinct subgroups, depending on the conformation of the tetracarboxylate ligand used. When the four carboxylates are arranged to form a square/rectangle, and if the SBL is based on the **sql-1**, or **sql-2** layer, the resulting 3-periodic structures will be an **ssb**-MOF<sup>192</sup> or an **lvt**-MOF, respectively,<sup>39</sup> if the SBL is based on the **kgm** layer, the result is, in most cases, an **nbo**-MOF.<sup>192–196</sup>

However, other L-L pillaring types are possible but require the use of 4-c ligands with slightly different geometry.

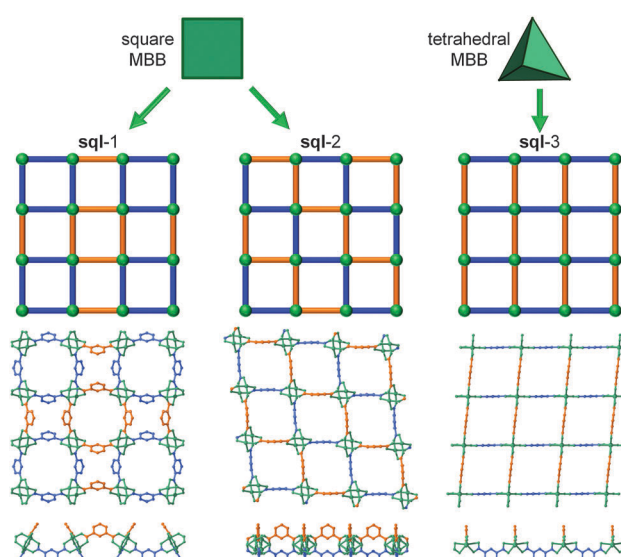
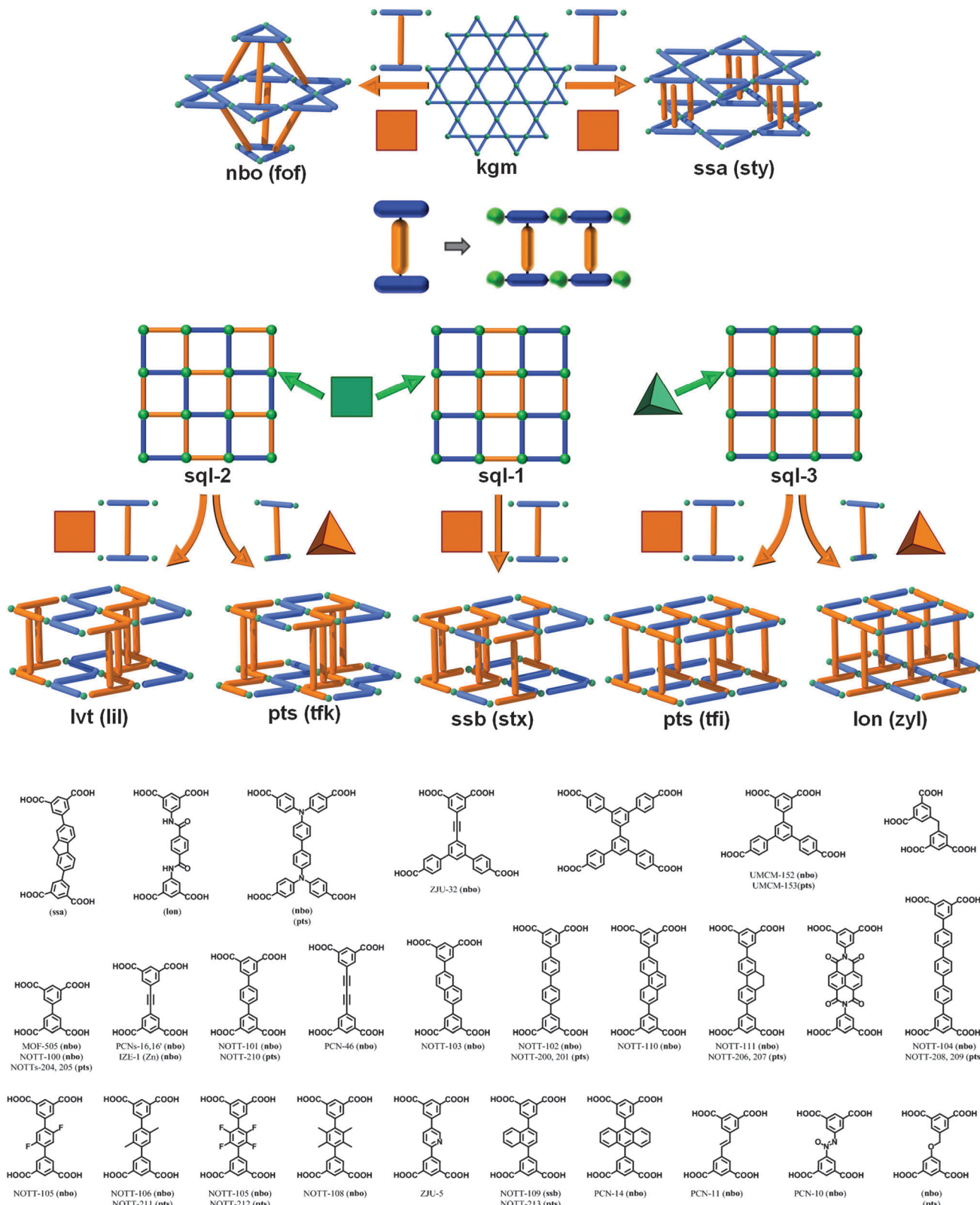


Fig. 29 Schematic representing three possible types of **sql** layer types that can be obtained with isophthalate and square paddlewheel MBBs (**sql-1** and **sql-2**) or isophthalate and tetrahedral indium MBBs (**sql-3**). Orange lines represent isophthalates pointing “up” while blue lines represent isophthalates pointing “down”.





**Fig. 30** Schematic of the L-L pillaring of **sql** and **kgm** layers to form the **nbo**, **ssa**, **lvt**, **pts**, **ssb**, and **lon** nets (top), and a non-exhaustive list of ligands that have been used for this type of pillaring (bottom).

Indeed, when **kgm** layers are produced by bent ligands such as isophthalate, the bent/functionalizable position of the ligand does

not point straightly up or down from the layer, but it is also oriented to point either inside or outside a specific window in the layer.

Depending on the orientation of the bent position, an additional topology, **ssa** (which can alternatively be described as **sty** if the 4-c ligand is considered as two 3-c nodes<sup>58</sup>), is possible.<sup>63,197</sup> In the reported examples, the tetracarboxylate ligands are not linear, this allows the geometry to deviate from the aforementioned predefined orientation of the isophthalate moieties (similarly to the rare cases of formation of **ssb**-MOFs).

When the four carboxylates from the ligand form a tetrahedron ( $D_{2d}$  symmetry; for example, two staggered isophthalates), the possible alternate pillaring of **sql-2** layers will lead to MOFs with the **pts** topology (which can alternatively be described as **tfk**, if the 4-c ligand is considered as two 3-c nodes<sup>58</sup>). To the best of our knowledge, no **tfk**-MOFs based on pillaring of **sql-2** SBLs have been reported so far.

It should be mentioned that, in addition to tuning the functionality of the ligand,<sup>192</sup> it is also possible to tune the cavities through use of relatively low symmetry (sometimes called asymmetric due to lack of a center of inversion) ligands. Indeed, in 2010, Matzger *et al.* reported the synthesis of an **nbo**-MOF (UMCM-152) and a **pts**-MOF (UMCM-153), where the **kgm** and **sql** layers are of a lower symmetry (Fig. 31). For the **kgm**, half of the triangle windows are constructed from isophthalate moieties, whereas the other half are made from the extended isophthalate analogue, benzene-dibenzoate. Regarding the **sql** structure, the square shape of the windows is now modified into a rectangular shape, delimited by two isophthalate and two benzene-dibenzoate moieties.<sup>198</sup> A similar strategy has recently been used by Qian *et al.* for the synthesis of an **nbo**-MOF (ZJU-32).<sup>199</sup>

Schröder *et al.* reported a series of pillared In-tetracarboxylate MOFs, where the layer is **sql-3**. In these cases, the two isophthalate moieties from the ligands are eclipsed, resulting in MOFs with **pts** topology.<sup>200–204</sup> At this stage, it is important to notice that two different **sqls** (**sql-2** and **sql-3**) can be pillared using the same type of pillaring (L-L) and lead to similar **pts** topology. This fact is actually due to the nature of the 4-c **pts** net, which results (in its augmented form) in the assembly of squares and tetrahedra. The **pts** net (Fig. 32) can then be regarded as (i) **sql-2** layers (based on square MBBs) pillared by tetrahedra (staggered 4-c ligands), or alternatively as (ii) **sql-3** layers (based on tetrahedral MBBs) pillared by square (eclipsed 4-c ligands). Interestingly, the expansion of the ligand for each case will lead

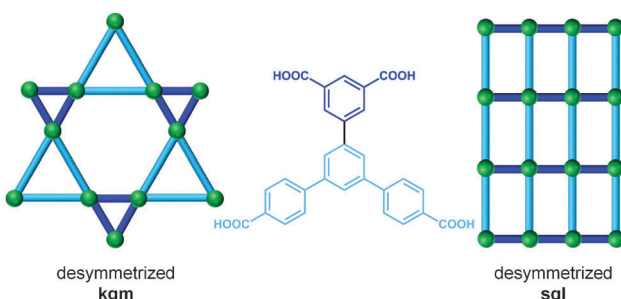


Fig. 31 Lower symmetry ligand strategy for the formation of a pillared **nbo**-MOF (UMCM-152) based on the asymmetric **kgm** layer and a **pts**-MOF (UMCM-153) based on lower symmetry **sql**.

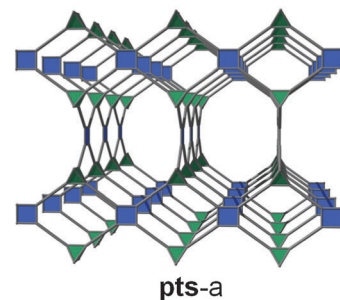


Fig. 32 View of the **pts** net. It can be regarded as both **sql-2** pillared by tetrahedra and **sql-3** pillared by squares.

to the expansion of the **pts** structure in two distinct ways. This difference will be well-reflected by using an alternative way of describing those structures, which consists of describing each 4-c ligand as two 3-c nodes<sup>58</sup> and permits us to differentiate the two types of structure. Then, the **pts** net from **sql-2** becomes a **tfk** net, while the **pts** net from **sql-3** becomes a **tfi** net.

The **pts** net is not the only one that can be achieved by L-L pillaring of **sql-3**. Indeed, Lah *et al.* recently reported a MOF where the  $\text{Co}_2(\text{O}_2\text{CR})_4(\text{H}_2\text{O})_3$  MBB has the shape of a tetrahedron, which are linked together by isophthalate moieties from the ligand to form an **sql-3** SBL. The second isophthalate moiety of the ligand is staggered (4-c ligand is then considered as a tetrahedron), resulting in a MOF with a very rare **lon** topology which can alternatively be described as **zyl**, if the 4-c ligand is considered as two 3-c nodes.<sup>58,204–206</sup>

### 3.3. **eea**-MOFs, **rtl**-MOFs, and other trigonal type pillaring

A third strategy (Fig. 33), comparable to the one previously mentioned in the SBB section for the construction of **txt**-MOFs, combines both of the previous two strategies through incorporating two types of function within the “linear” pillar molecule, a function that can interact with an accessible metal site on the one hand and the organic bridging ligand on the other hand. Thus, each ligand/pillar is a bi-functional ligand having trigonal geometry, containing a ditopic bridging moiety (e.g., 5-substituted isophthalate) that forms the expected MOF layer (e.g., **sql** or **kgm**),<sup>207,208</sup> as well as a second functional group (e.g., an N-donor group attached at the 5-position of isophthalate) allowing coordination to a metal site in a neighboring layer. This combination results in what the Eddaoudi group termed ligand-to-axial (L-A) pillaring. L-A pillaring, utilizing a trigonal (3-c) pillar, produces layers composed of bridged octahedral-like

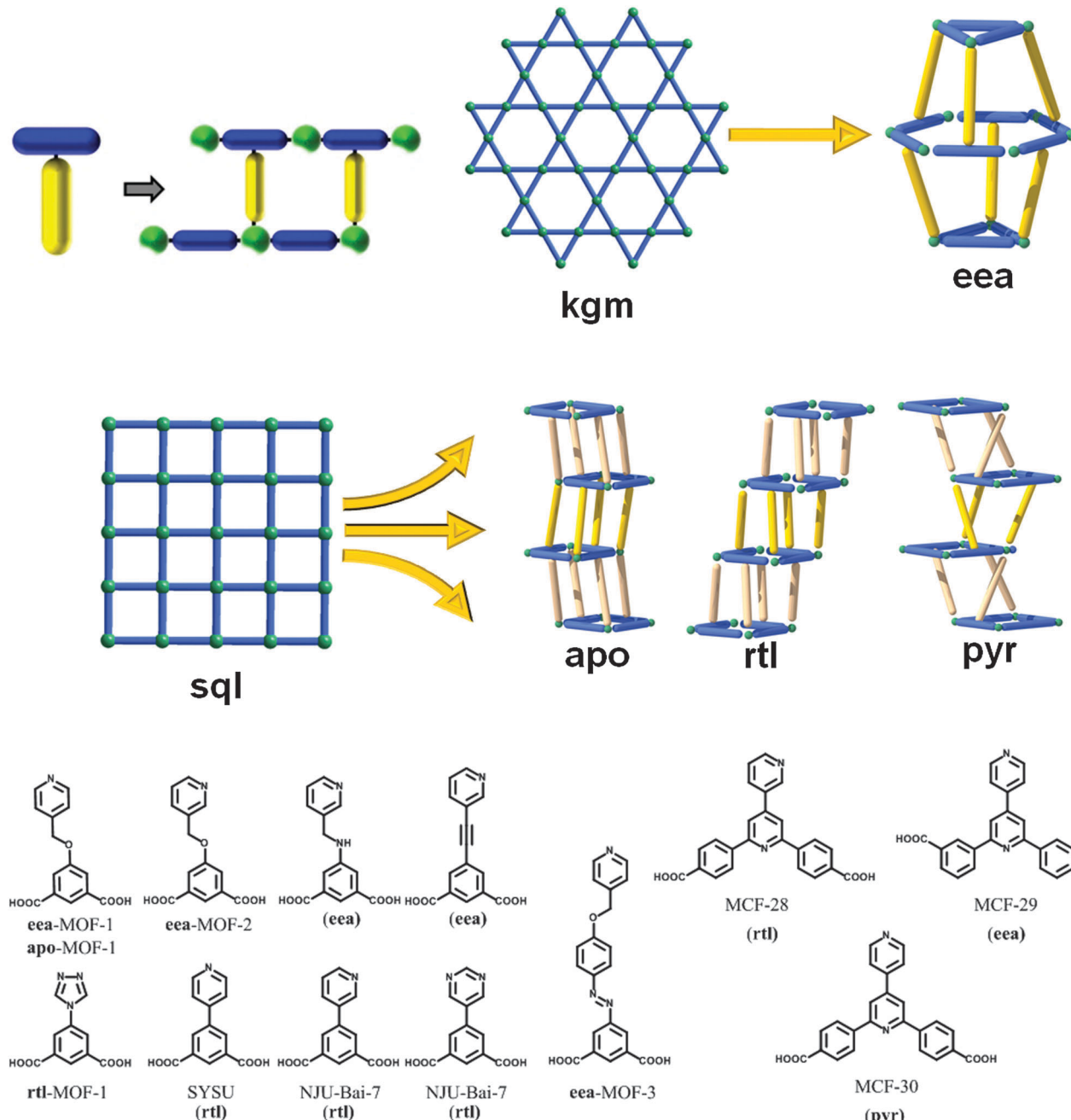


Fig. 33 Schematic of the different L–A trigonal pillaring types successfully targeted with **kgm** and **sql** layers (top). Non-exhaustive list of ligands used for trigonal, L–A, pillaring (bottom).

MBBs (6-c) building units, Fig. 33, and thus results in the construction of (3,6)-c, 3-periodic MOFs.

According to the RCSR database,<sup>9</sup> there were fifty one reported (3,6)-c nets at the time of our research, only six of which (*i.e.*, **anh**, **ant**, **apo**, **brk**, **pyr**, **rtl**), to our knowledge, can be deconstructed into 2D **sql** layers of octahedra linked by triangles (“Y”- or “T”-shaped). As such, these networks would be regarded as the most plausible targets using our strategy. The 2D layers in these targetable topologies correspond to the edge-transitive **sql** network, and as mentioned previously, edge-transitive nets are the most appropriate targets in crystal chemistry.

Utilizing this method, Eddaoudi and coworkers were able to design and utilize a relatively rigid bifunctional trigonal ligand, 5-(4H-1,2,4-triazol-4-yl)-isophthalic acid; reacting this ligand with copper salts allowed formation of the necessary paddlewheel MBB resulting in a targeted L–A pillared **sql**-MOF. Topological analysis of the resultant (3,6)-c net revealed an **rtl**-MOF.<sup>209</sup> This was the expected result as the rutile net (**rtl**) has been considered the “easiest target for a designed synthesis” for combining triangles and octahedra.<sup>210</sup> To the best of our knowledge, prior to this, only one similarly pillared **rtl**-MOF was reported, by Su *et al.* although no reference to pillaring was

mentioned, and the topology was not assigned as **tbo**.<sup>211</sup> Recent important contributions have also been reported in 2012 by Bai *et al.*<sup>212</sup>

To target the other (3,6)-c nets, it is possible to purposely introduce some flexibility into the pillar ligand *via* a methoxy linkage (e.g., 3- or 4-pyridylmethoxyisophthalic acid). This approach was reported by Eddaoudi's group to allow the intended formation of the first **apo**-MOF.<sup>209</sup> Expansion of the ligand allows the synthesis of 3-periodic MOFs with larger, non-interpenetrated cavities/pores. Additionally, it is also possible to form a (3,6)-c net from the 2-periodic supramolecular isomer, **kgm** SBL. Though not originally listed in the RCSR database, this additional (3,6)-c net was retroactively added, resulting in the existence of the first net (**eea**) based on the trigonal pillaring of **kgm** layers.<sup>209</sup> Notably, some isoreticular **eea**-MOFs, one of them now comprised of a rigid ligand, were reported by Lah *et al.*<sup>213,214</sup> Finally, a recent report from Chen *et al.* showed the possibility to target such trigonally-pillared MOFs by using expanded layers (*i.e.*, replacing isophthalate by pyridine-dibenzoate), including the one having **pyr** topology (MCF-30).<sup>215</sup>

### 3.4. Four-connected L-L pillars and **sql** layers: **tbo**, **mmm**, **bor**, **eed**, **ofp**, and **hge** nets

The fourth SBL approach was developed as a result of the understanding of the 3-dimensional nature of 3-periodic MOF structures and the design and development of corresponding complex multi-dimensional ligands. HKUST-1, one of the first prototype 3-periodic MOFs,<sup>216</sup> is well-known to be a (3,4)-c structure with **tbo** topology (*i.e.*, **tbo**-MOF) based on the trigonal (3-c) 1,3,5-BTC ligand and the square (4-c) paddlewheel dicopper MBB. Analogous or pyridyl-based expanded **tbo**-MOFs (based on trigonal ligands) have been widely studied,<sup>217–223</sup> and some of them are subject to interpenetration.<sup>218,221,222</sup>

Further analysis by the Eddaoudi group revealed that HKUST-1 can be deconstructed into **sql** layers that are cross-linked by a 4-c MBB. Thus, it can be envisioned that substitution of this MBB by analogous quadrangular organic MBBs (*i.e.*, a non-linear, octatopic, tetrafunctional, quadrangular pillar) will allow the formation of analogous layer-based, HKUST-analogous **tbo**-MOFs (Fig. 34–36).

Again, the modularity of this approach allowed for the facile development of a series of isoreticular MOFs with expansion of the distance between the layers, from 11 Å in HKUST-1 up to 27 Å in **tbo**-MOF-4.<sup>98</sup> Indeed, the ability to generate  $[M(R-BDC)]_n$  SBLs (in this case, **sql** is the **net**-CBU) consistently *in situ* and space them using organic pillars permits the relatively small square windows of the SBLs to be preserved. This, unlike in the non-(SBL-based) HKUST analogues, prevents self-interpenetration, but still allows the functionalization and/or enlargement of the cavities delimited by the pillars. This is especially interesting in the case of **tbo**-MOF-3, where additional carboxylic acid moieties were introduced as pendant groups on the quadrangular pillar used for **tbo**-MOF-2, and thus permitted construction of a **tbo**-MOF with pores/channels decorated by a periodic array of free carboxylic acid groups (Fig. 37). This designed feature is of particular interest, because it is, in fact, quite difficult to achieve in MOFs, as carboxylic acids and/or carboxylates

usually coordinate to the metals/clusters within the framework; this confirms the power of the SBL approach for the design and construction of “functional” MOFs. In addition, this functionalization in **tbo**-MOF-3 has an important impact on the gas sorption properties, as it allows, for example, the enhancement of the heats of adsorption for  $CO_2$  from 30 to 35 kJ mol<sup>-1</sup>,<sup>98</sup> but also gives rise to drastically enhanced hydrocarbon separation properties.<sup>99</sup>

It should be noted that since the introduction of the SBL approach to HKUST-1-like **tbo**-MOFs, several other examples in the **tbo**-MOF family have appeared in the open literature;<sup>224–226</sup> some of them (*e.g.*, ZJU-18-20), however, are composed of a slightly different **sql** SBL, half of the square MBBs forming the **sql** layer being a 4-c  $Mn_3(-O_2CR)_4(\mu-H_2O)$  trimer instead of the usual  $M_2(-O_2CR)_4$  paddlewheel.<sup>227</sup>

Another interesting example is illustrated by PCN-80. Indeed, this MOF is a **tbo**-MOF, but unlike most of the other examples, its “fully deconstructed” topology can be interpreted as a (3,3,4)-c net with **lwg** topology. Surprisingly, in this MOF/net, distance between the triangles (denoted “a” in Fig. 38) is closely related to the distance between the two carboxylates on each arm of the ligand (denoted “b”), which makes further expansion of the ligand very difficult, if not impossible in PCN-80, whereas ligand expansion is an easily achievable feature in some of the other reported **tbo**-MOFs.<sup>98</sup> However, one can imagine a net related to **tbo**, in which the deconstruction of the square/rectangle into two triangles<sup>58</sup> leads to a distance “a” independent from the distance “b”, making therefore the hypothetical MOFs obtained in this net expandable on the “a” distance without restriction of the “b” distance. We envisioned such a (3,3,4)-c net with transitivity [3333] (coordination sequence for each node: A: 4 8 16 24 42 64 84 108 132 174; B: 3 6 14 27 42 55 78 120 149 156; C: 3 8 13 24 38 59 81 102 135 167) and named it **gex**.

The second possible complex pillaring of **sql** SBLs (*i.e.*, by a tetragonal pillar) can be achieved by switching from square/rectangle pillar geometry to a geometrically tetrahedral pillar type, which will afford MOFs with **mmm** topology (Fig. 34 and Fig. 39). Lin *et al.* reported in 2009 the first examples of such a pillared **mmm**-MOF (which can be alternatively described as **mml** topology, while considering the tetrahedral shape as two staggered 3-c nodes<sup>58</sup>).<sup>228</sup> Since this early report, which did not refer to layers or pillaring, only a few more recent examples of **mmm**-MOFs have been reported, indicating that this pillaring type still lends to further exploration.<sup>229,230</sup>

The two previous types of pillaring are achieved using the **sql** layer denoted **sql-1** in Fig. 29. Of course, there might be other possible ways to pillar **sql** layers using squares or triangles that will involve **sql-2**. Due to the lack of information present in the literature, **sql-2** will not be discussed further in this review. However, another famous topology, namely boracite (**bor**), can, as the names suggest, be seen as related to **tbo** (twisted boracite). Using our SBL approach, it is obvious that MOFs having **bor** topology can be achieved through tetrahedral pillaring of **sql-3**.

Though it may not be the SBL approach, it is worth mentioning (in a review on SBBs as well) that the networks with both **tbo** and **bor** topologies can also be seen as based on the



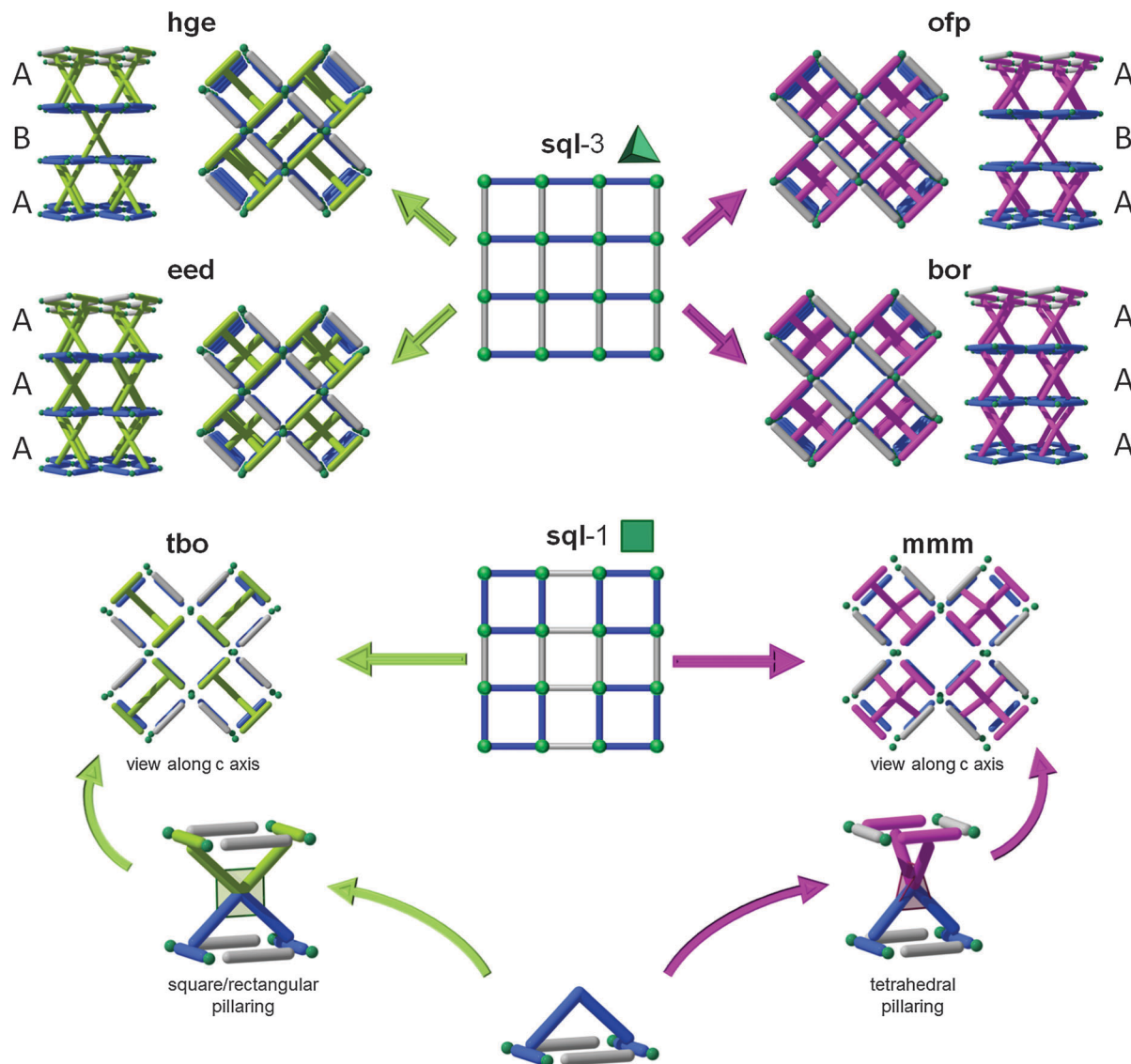


Fig. 34 Schematic of the pillaring of **sq1** layers by square/rectangle (left) and tetrahedral pillars (right).

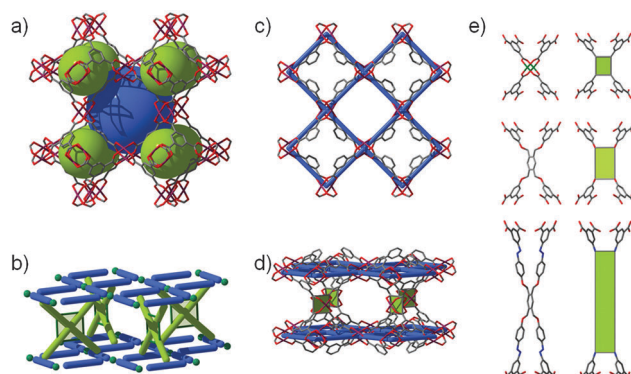


Fig. 35 (a) HKUST-1 (**tbo**-MOF-1), the **tbo**-MOF prototype. (b) Schematic showing the **tbo** net. (c) Highlight of the **sq1** layer in HKUST-1. (d) Highlight of the pillared **sq1** (**tbo** net) in HKUST-1. (e) Representation of the achieved expansion of the quadrangular pillar in **tbo**-MOFs.

edge-center-shared tetrahedral MOPs (Fig. 40). While the shared edge-center in **tbo** net is a planar 4-c node of  $D_{2h}$  point symmetry, the corresponding shared edge-center in the **bor** net is a tetrahedral 4-c node of  $D_{2d}$  point symmetry.

Several MOFs with the **bor** topology have been reported (Fig. 41),<sup>231–236</sup> but, to the best of our knowledge, there are only a limited number of **bor**-MOFs where the net is constructed from the pillaring of **sq1** by tetrahedra, that is, MOFs where the tetrahedra form the **sq1** are distinct from the tetrahedra that serve as pillars (*i.e.*, only a few SBL-based **bor**-MOFs).<sup>237,238</sup>

Interestingly, and comparable to the case of **rtl** and **apo** nets (Fig. 33), two distinct ways are possible for this type of pillaring of **sq1**, leading to a second topology, namely **ofp**.<sup>239</sup> This **ofp** net can be regarded as A-B-A pillaring of **sq1**s, whereas the **bor** net is of the A-A-A pillaring type (Fig. 34). Since the **ofp** net is not an edge-transitive net, it is not as favorable in crystal chemistry and is less likely to be observed than the **bor** net.



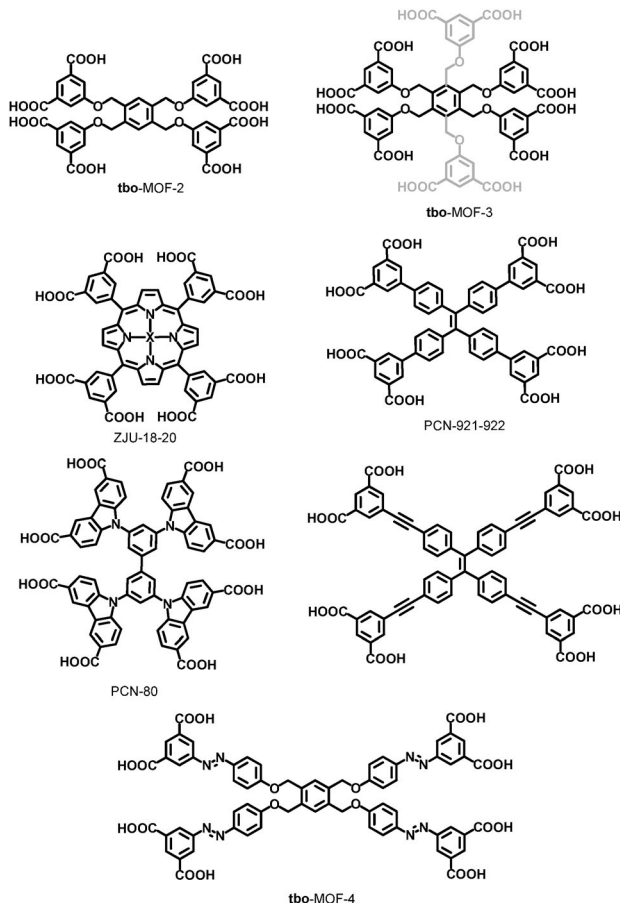


Fig. 36 Non-exhaustive list of square/rectangle ligands utilized for the SBL formation of **tbo**-MOFs. Gray part of the **tbo**-MOF-3 ligand corresponds to non-coordinating isophthalic acid moieties.

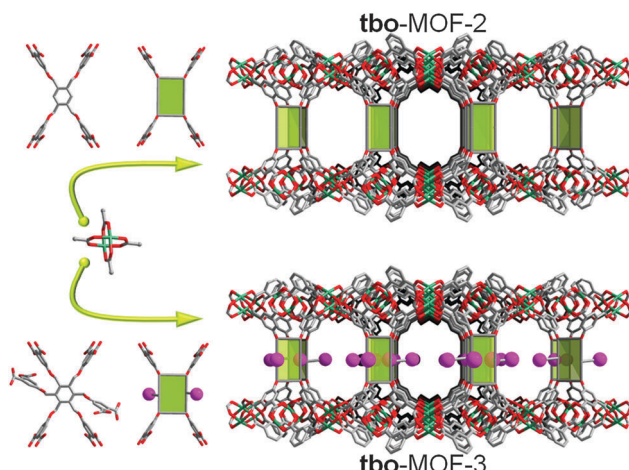


Fig. 37 Illustration of the ease of functionalization of the central core of **tbo**-MOFs.

Similar to the case of **tbo** and **mmm** from **sql-1**, not only can the **sql-3** layer be pillared by tetrahedra, as described above, but also by squares/rectangles. Likewise, two distinct ways are possible for this type of pillaring, leading to two distinct

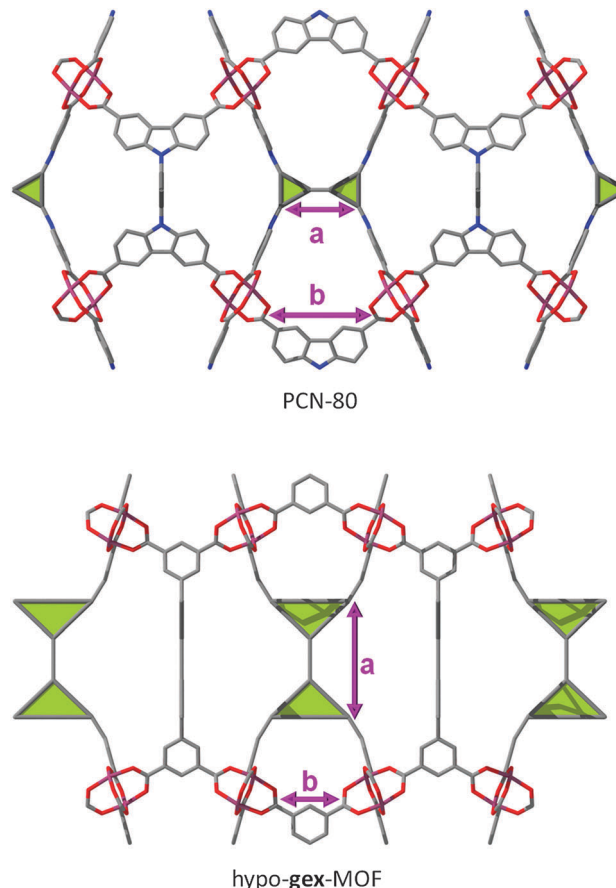


Fig. 38 Comparison of the expandability in **lgw**-MOFs and **gex**-MOFs.

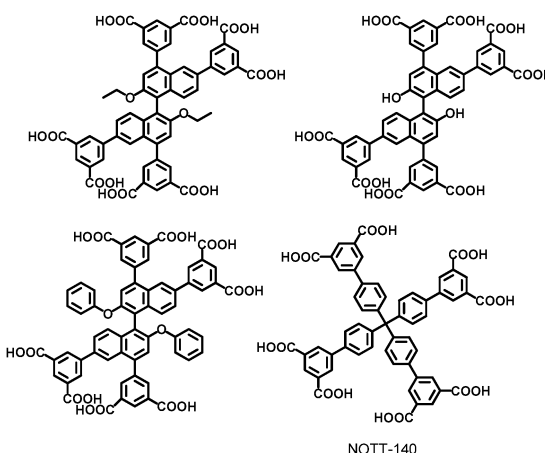


Fig. 39 Non-exhaustive list of tetrahedral ligands used to produce **mmm**-MOFs.

(3,4,4)-c nets that had not been reported prior to this review. The first topology, now added to the RCSR as **eed**, corresponds to a (3,4,4)-c net with transitivity [3221] (coordination sequence for each node: A: 3 9 15 33 45 82 90 153 150 230; B: 4 8 20 30 60 68 120 126 200 180; C: 4 8 20 30 60 68 120 126 200 180) and consists of A-A-A pillaring, whereas the second topology, **hge** corresponds to a (3,4,4)-c net with transitivity [3221]

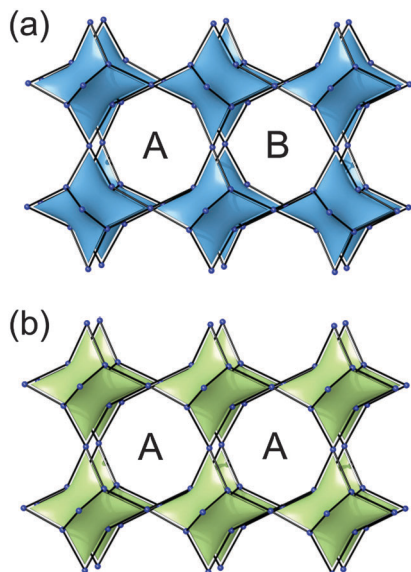


Fig. 40 A comparison of the two (3,4)-c nets with (a) **tbo** topology and (b) **bor** topology based on edge-center-shared tetrahedral MOPs.

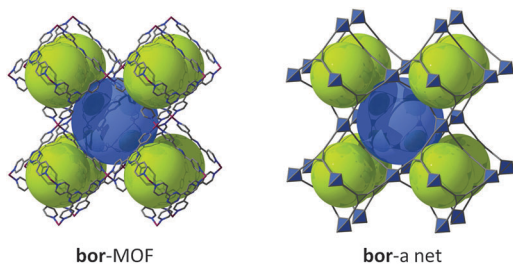


Fig. 41 View of a **bor**-MOF and the related **bor** net (shown as augmented).

(coordination sequence for each node: A: 3 9 15 33 44 80 86 147 142 229; B: 4 8 20 28 56 68 120 110 184 188; C: 4 8 20 30 60 64 112 118 192 172) and A-B-A pillararing (Fig. 34). At the time of our research, no MOFs having these topologies have been reported, but there is no doubt such MOFs can be reasonably targeted and achieved using the SBL approach and the appropriate metal-ligand systems.<sup>240</sup>

### 3.5. Six-connected L-L pillars and **kgm** layers: **agw** and **eef** nets

Due to the symmetry of the quadrangular- and tetrahedral-core pillars, **kgm** layers (with triangular and hexagonal pores) have been precluded from the previous two examples of the SBL approach. Nonetheless, **kgm** SBLs can also be utilized to target 3-periodic MOFs with multi-dimensional ligands of different symmetry (*e.g.*,  $O_h$  and  $D_{3h}$ ). There are two common types of 6-c node, octahedral and trigonal prism, which could serve as a multi-connected pillar between **kgm** layers. If we explore the paddlewheel-based **kgm**-MOF, one can envision how a hexa-isophthalate ligand or metalloligand (3-up, 3-down) might serve the purpose to target pillared **kgm**-MOFs. While the isophthalates, in combination with the  $M_2(-O_2CR)_4$  dinuclear

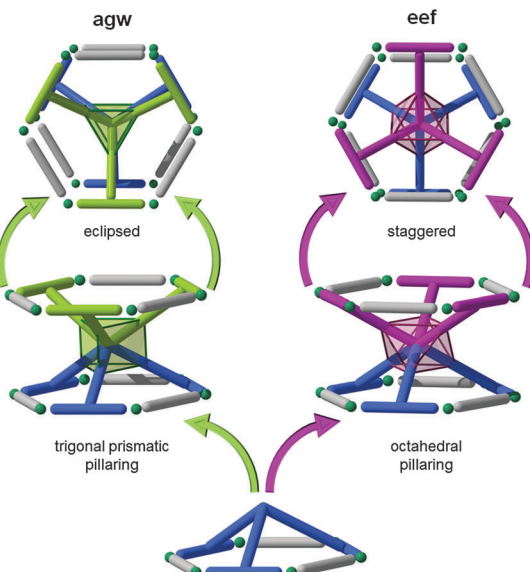


Fig. 42 Schematic showing the two possible ways for hexatopic pillaring of **kgm** layers. Trigonal prism (left) or octahedral (right) pillared **kgm**-MOFs can be obtained by using the appropriate pillaring ligand/molecule.

paddlewheel cluster, generate the two-periodic **kgm** SBL, functionalization in the isophthalate 5-position, either through covalent linkage to a 6-c organic core (*e.g.*, hexa-substituted benzene) or to an ancillary function that can coordinate to a 6-c metal/cluster (*e.g.*, metalloligand), offers the potential to generate numerous cross-linked **kgm**-MOFs (Fig. 42).

A review of the CSD<sup>97</sup> reveals that hexa-substituted benzenes often give a 3-up, 3-down orientation of the external groups. Thus, the design and synthesis of a hexa-isophthalate ligand, similar to the one used for the carboxylate-functionalized **tbo**-MOF-3, has the potential to give an octahedral organic core, covalently linking each of the six isophthalate termini resulting in an octahedral orientation; this feature combined with the **kgm** SBL results in a net with the recently added **eef** topology.<sup>240</sup>

Alternatively, the pillaring of **kgm** through a trigonal prismatic core results in a net having **agw** topology (*i.e.*, **agw**-MOFs). Though obviously predictable *via* the SBL approach, this type of structure was first discovered serendipitously by employing lower symmetry tricarboxylate (*i.e.*, pseudo-heterofunctional) ligands in combination with metals suitable for formation of the dinuclear paddlewheel MBB (*e.g.*, copper). However, an additional MBB, an unexpected trinuclear cluster, formed *in situ*, which, in combination with the ligand, mimics a trigonal prism hexa-isophthalate ligand, and, with the paddlewheel, this “metalloligand” gave rise to the corresponding pillared **kgm**-MOF, an **agw**-MOF. To the best of our knowledge, no reference to any pillaring technique was mentioned.<sup>241</sup> Similar materials have since been retroactively targeted and achieved by utilizing a mixed-metal system, where a secondary metal (copper being the primary metal which forms the paddlewheel and the SBLs) is utilized to form a trinuclear trigonal prism cluster MBB as the core of the metalloligand pillar.<sup>242</sup>



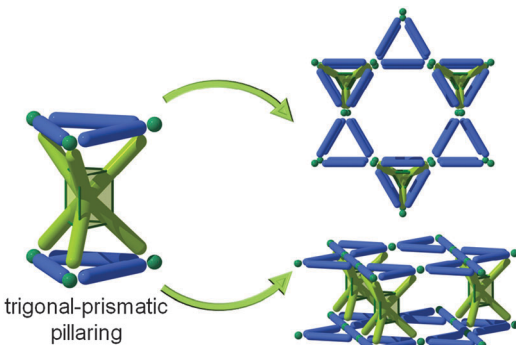


Fig. 43 Schematic showing the possible axial-to-axial (A-A) pillaring of **kgm** layers by trigonal prism pillars, leading to **ion-e** topology.

### 3.6. Six-connected A-A pillars and kgm layers: ion-e net

As the last example of pillared MOFs using the SBL strategy (A-A fashion, Fig. 43), Zaworotko *et al.* recently developed a stepwise path for the achievement of a similar type of pillaring.<sup>243</sup> Rather than targeting conditions to form the requisite trigonal prism *in situ*, their group developed relatively stable trinuclear trigonal prism clusters (*i.e.*, discrete) from chromium salts with the formula  $\text{Cr}_3(\mu_3\text{O})(-\text{O}_2\text{CR})_6$ , decorated by six pyridyl moieties. They were then able to target the **kgm** SBL *in situ* for the construction of a series of pillared MOFs with **ion-e** topology. This method broadens the scope of the SBL approach and pillaring strategies toward the design of functional materials.

### 3.7. Layers for MOFs: Conclusion

As demonstrated above, the SBL approach relies on the use of a metal–organic layer, usually based on edge-transitive lattices (*e.g.*, Kagomé and square), as an elaborate building entity (the **net-cBU**, in this case) that is then periodically cross-linked (pillared) into predicted three-periodic MOFs. Once the **net-cBU** is established, pillaring can be targeted via three different methods, depending on the the SBL and respective geometry (*e.g.*, bridging ligand orientation): (1) Axial-to-axial (A-A); (2) axial-to-ligand (A-L); and (3) ligand-to-ligand (L-L), which can be subdivided into simple (*e.g.*, linear) or complex (*e.g.*, multi-dimensional). As in the case of SBBs, the key prerequisites to use the SBL approach for the design of a MOF are: (1) A blueprint net with minimal edge-transitivity, preferably singular, that is exclusive for the particular pillaring of the given building units, and (2) reaction conditions that permit us to consistently form the desired SBL *in situ*. Uniquely, control of the SBL pores allows the material designer to preclude self-interpenetration upon net expansion and/or decoration, leading to predicted and unprecedented MOFs with tunable cavities, essentially isoreticular platforms that can be ideally functionalized for pressing applications pertaining to catalysis and gas separation.

## 4. Conclusions

In this review, we described and illustrated two powerful design strategies, namely the SBB and SBL approaches. Without being

exhaustive, we carefully selected relevant examples that should guide researchers and show them how judicious selection of pre-programmed SBBs or SBLs allows for the construction of pre-designed MOFs.

Although topological considerations are of prime importance to describe the structure, we encourage chemists to use the tools of topology (net, connectivity, edge-transitivity, minimal transitivity) to elucidate the ideal SBBs or SBLs with all the coded structural/geometrical information that will serve as **net-cBUs** to construct the desired MOFs.

To illustrate these methodologies, we described some topologies for which MOFs have already been reported, but also proposed some new ideas (*i.e.*, some unprecedented topologies) that have not yet been explored. There is no doubt they are attainable targets in MOF chemistry, as they are envisioned from the assembly of already existing SBLs or SBBs.

Finally, using an ideal blueprint, in combination with the appropriate pre-programmed SBB or SBL, design almost becomes a reality, and the only limitation for the construction of the desired functional MOFs is the chemist/material designer's imagination.

## Acknowledgements

This work was supported by the King Abdullah University of Science and Technology (KAUST). NRF-2010-0019408 and NRF-2012R1A2A2A01003077 through the National Research Foundation of Korea.

## Notes and references

- 1 M. Eddaoudi, D. B. Moler, H. L. Li, B. L. Chen, T. M. Reineke, M. O'Keeffe and O. M. Yaghi, *Acc. Chem. Res.*, 2001, **34**, 319–330.
- 2 G. Férey, *Chem. Soc. Rev.*, 2008, **37**, 191–214.
- 3 Z.-J. Lin, J. Lu, M. Hong and R. Cao, *Chem. Soc. Rev.*, 2014, DOI: 10.1039/c4cs00003j.
- 4 W. Lu, Z. Wei, Z.-Y. Gu, T.-F. Liu, J. Park, J. Park, J. Tian, M. Zhang, Q. Zhang, T. Gentle Iii, M. Bosch and H.-C. Zhou, *Chem. Soc. Rev.*, 2014, DOI: 10.1039/c4cs00041b.
- 5 M. Eddaoudi, J. Kim, N. Rosi, D. Vodak, J. Wachter, M. O'Keeffe and O. M. Yaghi, *Science*, 2002, **295**, 469–472.
- 6 S. M. Cohen, *Chem. Rev.*, 2012, **112**, 970–1000.
- 7 J. R. Long, O. M. Yaghi, (ed.) *Chem. Soc. Rev.*, 2009, **38**, 1201–1508.
- 8 H. C. Zhou, J. R. Long, O. M. Yaghi, (ed.) *Chem. Rev.*, 2012, **112**, 673–1268.
- 9 M. O'Keeffe, M. A. Peskov, S. J. Ramsden and O. M. Yaghi, *Acc. Chem. Res.*, 2008, **41**, 1782–1789.
- 10 V. Guillerm, L. J. Weselinski, Y. Belmabkhout, A. J. Cairns, V. D'Elia, L. Wojtas, K. Adil and M. Eddaoudi, *Nat. Chem.*, 2014, DOI: 10.1038/NCHEM.1982.
- 11 D.-X. Xue, A. J. Cairns, Y. Belmabkhout, L. Wojtas, Y. Liu, M. H. Alkordi and M. Eddaoudi, *J. Am. Chem. Soc.*, 2013, **135**, 7660–7667.



12 J. F. Eubank, F. Nouar, R. Luebke, A. J. Cairns, L. Wojtas, M. Alkordi, T. Bousquet, M. R. Hight, J. Eckert, J. P. Emb, P. A. Georgiev and M. Eddaoudi, *Angew. Chem., Int. Ed.*, 2012, **51**, 10099–10103.

13 F. Nouar, J. F. Eubank, T. Bousquet, L. Wojtas, M. J. Zaworotko and M. Eddaoudi, *J. Am. Chem. Soc.*, 2008, **130**, 1833–1834.

14 W. Morris, B. Voloskiy, S. Demir, F. Gandara, P. L. McGrier, H. Furukawa, D. Cascio, J. F. Stoddart and O. M. Yaghi, *Inorg. Chem.*, 2012, **51**, 6443–6445.

15 J. H. Cavka, S. Jakobsen, U. Olsbye, N. Guillou, C. Lamberti, S. Bordiga and K. P. Lillerud, *J. Am. Chem. Soc.*, 2008, **130**, 13850–13851.

16 V. Guillerm, S. Gross, C. Serre, T. Devic, M. Bauer and G. Férey, *Chem. Commun.*, 2010, **46**, 767–769.

17 V. Guillerm, F. Ragon, M. Dan-Hardi, T. Devic, M. Vishnuvarthan, B. Campo, A. Vimont, G. Clet, Q. Yang, G. Maurin, G. Férey, A. Vittadini, S. Gross and C. Serre, *Angew. Chem., Int. Ed.*, 2012, **51**, 9267–9271.

18 M. Dan-Hardi, C. Serre, T. Frot, L. Rozes, G. Maurin, C. Sanchez and G. Férey, *J. Am. Chem. Soc.*, 2009, **131**, 10857–10859.

19 D.-Y. Du, J.-S. Qin, Z. Sun, L.-K. Yan, M. O'Keeffe, Z.-M. Su, S.-L. Li, X.-H. Wang, X.-L. Wang and Y.-Q. Lan, *Sci. Rep.*, 2013, **3**, 2616.

20 R. Luebke, J. F. Eubank, A. J. Cairns, Y. Belmabkhout, L. Wojtas and M. Eddaoudi, *Chem. Commun.*, 2012, **48**, 1455–1457.

21 R. Luebke, L. J. Weseliński, Y. Belmabkhout, Z. Chen, L. Wojtas and M. Eddaoudi, *Cryst. Growth Des.*, 2014, **14**, 414–418.

22 U. Stoeck, S. Krause, V. Bon, I. Senkovska and S. Kaskel, *Chem. Commun.*, 2012, **48**, 10841–10843.

23 A. J. Cairns, J. A. Perman, L. Wojtas, V. C. Kravtsov, M. H. Alkordi, M. Eddaoudi and M. J. Zaworotko, *J. Am. Chem. Soc.*, 2008, **130**, 1560–1561.

24 M. Eddaoudi, J. F. Eubank, F. Nouar, L. Wojtas, T. Bousquet and M. J. Zaworotko, US2009143596-A1, US8034952-B2, 2009.

25 Y. L. Liu, V. Kravtsov, R. D. Walsh, P. Poddar, H. Srikanth and M. Eddaoudi, *Chem. Commun.*, 2004, 2806–2807.

26 M. H. Alkordi, J. A. Brant, L. Wojtas, V. C. Kravtsov, A. J. Cairns and M. Eddaoudi, *J. Am. Chem. Soc.*, 2009, **131**, 17753–17755.

27 M. O'Keeffe and O. M. Yaghi, *Chem. Rev.*, 2012, **112**, 675–702.

28 M. Li, D. Li, M. O'Keeffe and O. M. Yaghi, *Chem. Rev.*, 2014, **114**, 1343–1370.

29 N. W. Ockwig, O. Delgado-Friedrichs, M. O'Keeffe and O. M. Yaghi, *Acc. Chem. Res.*, 2005, **38**, 176–182.

30 D. J. Tranchemontagne, J. L. Mendoza-Cortes, M. O'Keeffe and O. M. Yaghi, *Chem. Soc. Rev.*, 2009, **38**, 1257–1283.

31 M. Eddaoudi, J. Kim, D. Vodak, A. Sudik, J. Wachter, M. O'Keeffe and O. M. Yaghi, *Proc. Natl. Acad. Sci. U. S. A.*, 2002, **99**, 4900–4904.

32 J. Bunzen, J. Iwasa, P. Bonakdarzadeh, E. Numata, K. Rissanen, S. Sato and M. Fujita, *Angew. Chem., Int. Ed.*, 2012, **51**, 3161–3163.

33 Q.-F. Sun, J. Iwasa, D. Ogawa, Y. Ishido, S. Sato, T. Ozeki, Y. Sei, K. Yamaguchi and M. Fujita, *Science*, 2010, **328**, 1144–1147.

34 M. Eddaoudi, J. Kim, J. B. Wachter, H. K. Chae, M. O'Keeffe and O. M. Yaghi, *J. Am. Chem. Soc.*, 2001, **123**, 4368–4369.

35 B. Moulton, J. J. Lu, A. Mondal and M. J. Zaworotko, *Chem. Commun.*, 2001, 863–864.

36 Z. Ni, A. Yassar, T. Antoun and O. M. Yaghi, *J. Am. Chem. Soc.*, 2005, **127**, 12752–12753.

37 J.-R. Li, A. A. Yakovenko, W. Lu, D. J. Timmons, W. Zhuang, D. Yuan and H.-C. Zhou, *J. Am. Chem. Soc.*, 2010, **132**, 17599–17610.

38 J.-R. Li, D. J. Timmons and H.-C. Zhou, *J. Am. Chem. Soc.*, 2009, **131**, 6368–6369.

39 H. Furukawa, J. Kim, N. W. Ockwig, M. O'Keeffe and O. M. Yaghi, *J. Am. Chem. Soc.*, 2008, **130**, 11650–11661.

40 J.-R. Li and H.-C. Zhou, *Angew. Chem., Int. Ed.*, 2009, **48**, 8465–8468.

41 T. R. Cook, Y.-R. Zheng and P. J. Stang, *Chem. Rev.*, 2013, **113**, 734–777.

42 R. Chakrabarty, P. S. Mukherjee and P. J. Stang, *Chem. Rev.*, 2011, **111**, 6810–6918.

43 J. J. Perry, J. A. Perman and M. J. Zaworotko, *Chem. Soc. Rev.*, 2009, **38**, 1400–1417.

44 A. C. Sudik, A. R. Millward, N. W. Ockwig, A. P. Côté, J. Kim and O. M. Yaghi, *J. Am. Chem. Soc.*, 2005, **127**, 7110–7118.

45 A. C. Sudik, A. P. Côté, A. G. Wong-Foy, M. O'Keeffe and O. M. Yaghi, *Angew. Chem., Int. Ed.*, 2006, **45**, 2528–2533.

46 G. Férey, C. Serre, C. Mellot-Draznieks, F. Millange, S. Surblé, J. Dutour and I. Margiolaki, *Angew. Chem., Int. Ed.*, 2004, **43**, 6296–6301.

47 G. Férey, C. Mellot-Draznieks, C. Serre, F. Millange, J. Dutour, S. Surblé and I. Margiolaki, *Science*, 2005, **309**, 2040–2042.

48 A. Sonnauer, F. Hoffmann, M. Froeba, L. Kienle, V. Duppel, M. Thommes, C. Serre, G. Férey and N. Stock, *Angew. Chem., Int. Ed.*, 2009, **48**, 3791–3794.

49 H. Chevreau, T. Devic, F. Salles, G. Maurin, N. Stock and C. Serre, *Angew. Chem., Int. Ed.*, 2013, **52**, 5056–5060.

50 C. Mellot-Draznieks, J. Dutour and G. Férey, *Z. Anorg. Allg. Chem.*, 2004, **630**, 2599–2604.

51 M. H. Alkordi, J. L. Belof, E. Rivera, L. Wojtas and M. Eddaoudi, *Chem. Sci.*, 2011, **2**, 1695–1705.

52 D. F. Sava, V. C. Kravtsov, J. Eckert, J. F. Eubank, F. Nouar and M. Eddaoudi, *J. Am. Chem. Soc.*, 2009, **131**, 10394–10395.

53 O. Delgado-Friedrichs, M. O'Keeffe and O. M. Yaghi, *Acta Crystallogr., Sect. A: Found. Crystallogr.*, 2006, **62**, 350–355.

54 R.-Q. Zou, H. Sakurai and Q. Xu, *Angew. Chem., Int. Ed.*, 2006, **45**, 2542–2546.

55 T. Wu, X. Bu, J. Zhang and P. Feng, *Chem. Mater.*, 2008, **20**, 7377–7382.

56 J.-Z. Chen, Y.-G. Tu, X.-L. Nie and H.-L. Wen, *Chin. J. Synth. Chem.*, 2011, **19**, 359.

57 Y. Liu, V. Ch. Kravtsov, D. A. Beauchamp, J. F. Eubank and M. Eddaoudi, *J. Am. Chem. Soc.*, 2005, **127**, 7266–7267.



58 J. F. Eubank, R. D. Walsh, P. Poddar, H. Srikanth, R. W. Larsen and M. Eddaoudi, *Cryst. Growth Des.*, 2006, **6**, 1453–1457.

59 M. O’Keeffe and B. G. Hyde, *Mineralogical Society of America*, Washington, DC, 1996.

60 J. J. Perry, V. C. Kravtsov, G. J. McManus and M. J. Zaworotko, *J. Am. Chem. Soc.*, 2007, **129**, 10076–10077.

61 C. Li, W. Qiu, W. Shi, H. Song, G. Bai, H. He, J. Li and M. J. Zaworotko, *CrystEngComm*, 2012, **14**, 1929.

62 X. Liu, M. Park, S. Hong, M. Oh, J. W. Yoon, J.-S. Chang and M. S. Lah, *Inorg. Chem.*, 2009, **48**, 11507–11509.

63 X.-S. Wang, S. Ma, P. M. Forster, D. Yuan, J. Eckert, J. J. López, B. J. Murphy, J. B. Parise and H.-C. Zhou, *Angew. Chem., Int. Ed.*, 2008, **47**, 7263–7266.

64 G. J. McManus, Z. Q. Wang and M. J. Zaworotko, *Cryst. Growth Des.*, 2004, **4**, 11–13.

65 H. Chun, *J. Am. Chem. Soc.*, 2008, **130**, 800–801.

66 H. Chun, H. Jung and J. Seo, *Inorg. Chem.*, 2009, **48**, 2043–2047.

67 H.-N. Wang, X. Meng, G.-S. Yang, X.-L. Wang, K.-Z. Shao, Z.-M. Su and C.-G. Wang, *Chem. Commun.*, 2011, **47**, 7128–7130.

68 O. Delgado-Friedrichs and M. O’Keeffe, *Acta Crystallogr., Sect. A: Found. Crystallogr.*, 2007, **63**, 344–347.

69 Y. Zou, M. Park, S. Hong and M. S. Lah, *Chem. Commun.*, 2008, 2340–2342.

70 B. Li, Z. Zhang, Y. Li, K. Yao, Y. Zhu, Z. Deng, F. Yang, X. Zhou, G. Li, H. Wu, N. Nijem, Y. J. Chabal, Z. Lai, Y. Han, Z. Shi, S. Feng and J. Li, *Angew. Chem., Int. Ed.*, 2012, **51**, 1412–1415.

71 D. Yuan, D. Zhao, D. Sun and H.-C. Zhou, *Angew. Chem., Int. Ed.*, 2010, **49**, 5357–5361.

72 D. Fairén-Jimenez, Y. J. Colon, O. K. Farha, Y.-S. Bae, J. T. Hupp and R. Q. Snurr, *Chem. Commun.*, 2012, **48**, 10496–10498.

73 S. Hong, M. Oh, M. Park, J. W. Yoon, J.-S. Chang and M. S. Lah, *Chem. Commun.*, 2009, 5397–5399.

74 Y. Peng, G. Srinivas, C. E. Wilmer, I. Eryazici, R. Q. Snurr, J. T. Hupp, T. Yildirim and O. K. Farha, *Chem. Commun.*, 2013, **49**, 2992–2994.

75 Y. Yan, X. Lin, S. Yang, A. J. Blake, A. Dailly, N. R. Champness, P. Hubberstey and M. Schroeder, *Chem. Commun.*, 2009, 1025–1027.

76 Y. Yan, S. Yang, A. J. Blake, W. Lewis, E. Poirier, S. A. Barnett, N. R. Champness and M. Schroeder, *Chem. Commun.*, 2011, **47**, 9995–9997.

77 B. Zheng, Z. Yang, J. Bai, Y. Li and S. Li, *Chem. Commun.*, 2012, **48**, 7025–7027.

78 D. Ma, B. Li, X. Zhou, Q. Zhou, K. Liu, G. Zeng, G. Li, Z. Shi and S. Feng, *Chem. Commun.*, 2013, **49**, 8964–8966.

79 Y. Yan, A. J. Blake, W. Lewis, S. A. Barnett, A. Dailly, N. R. Champness and M. Schroeder, *Chem. – Eur. J.*, 2011, **17**, 11162–11170.

80 I. Eryazici, O. K. Farha, B. G. Hauser, A. O. Yazaydin, A. A. Sarjeant, S. T. Nguyen and J. T. Hupp, *Cryst. Growth Des.*, 2012, **12**, 1075–1080.

81 W. Wei, W. Li, X. Wang and J. He, *Cryst. Growth Des.*, 2013, **13**, 3843–3846.

82 D. Yuan, D. Zhao and H.-C. Zhou, *Inorg. Chem.*, 2011, **50**, 10528–10530.

83 O. K. Farha, I. Eryazici, N. C. Jeong, B. G. Hauser, C. E. Wilmer, A. A. Sarjeant, R. Q. Snurr, S. T. Nguyen, A. Ö. Yazaydin and J. T. Hupp, *J. Am. Chem. Soc.*, 2012, **134**, 15016–15021.

84 C. E. Wilmer, O. K. Farha, T. Yildirim, I. Eryazici, V. Krungleviciute, A. A. Sarjeant, R. Q. Snurr and J. T. Hupp, *Energy Environ. Sci.*, 2013, **6**, 1158–1163.

85 G. Barin, V. Krungleviciute, D. A. Gomez-Gualdrón, A. A. Sarjeant, R. Q. Snurr, J. T. Hupp, T. Yildirim and O. K. Farha, *Chem. Mater.*, 2014, **26**, 1912–1917.

86 O. K. Farha, I. Eryazici, N. C. Jeong, B. G. Hauser, C. E. Wilmer, A. A. Sarjeant, R. Q. Snurr, S. T. Nguyen, A. Ö. Yazaydin and J. T. Hupp, *J. Am. Chem. Soc.*, 2012, **134**, 15016–15021.

87 O. K. Farha, A. O. Yazaydin, I. Eryazici, C. D. Malliakas, B. G. Hauser, M. G. Kanatzidis, S. T. Nguyen, R. Q. Snurr and J. T. Hupp, *Nat. Chem.*, 2010, **2**, 944–948.

88 P. Zhang, B. Li, Y. Zhao, X. Meng and T. Zhang, *Chem. Commun.*, 2011, **47**, 7722–7724.

89 J. Park, J. R. Li, Y. P. Chen, J. Yu, A. A. Yakovenko, Z. U. Wang, L. B. Sun, P. B. Balbuena and H. C. Zhou, *Chem. Commun.*, 2012, **48**, 9995–9997.

90 T.-T. Lian, S.-M. Chen, F. Wang and J. Zhang, *CrystEngComm*, 2013, **15**, 1036–1038.

91 J. Park, S. Hong, D. Moon, M. Park, K. Lee, S. Kang, Y. Zou, R. P. John, G. H. Kim and M. S. Lah, *Inorg. Chem.*, 2007, **46**, 10208–10213.

92 Z.-J. Zhang, W. Shi, Z. Niu, H.-H. Li, B. Zhao, P. Cheng, D.-Z. Liao and S.-P. Yan, *Chem. Commun.*, 2011, **47**, 6425–6427.

93 X. Zhao, X. Wang, S. Wang, J. Dou, P. Cui, Z. Chen, D. Sun, X. Wang and D. Sun, *Cryst. Growth Des.*, 2012, **12**, 2736–2739.

94 X.-R. Hao, X.-L. Wang, K.-Z. Shao, G.-S. Yang, Z.-M. Su and G. Yuan, *CrystEngComm*, 2012, **14**, 5596–5603.

95 J. J. Lu, A. Mondal, B. Moulton and M. J. Zaworotko, *Angew. Chem., Int. Ed.*, 2001, **40**, 2113–2116.

96 H. Li, M. Eddaoudi, T. L. Groy and O. M. Yaghi, *J. Am. Chem. Soc.*, 1998, **120**, 8571–8572.

97 F. H. Allen, *Acta Cryst.*, 2002, **B58**, 380–388.

98 J. F. Eubank, H. Mouttaki, A. J. Cairns, Y. Belmabkhout, L. Wojtas, R. Luebke, M. Alkordi and M. Eddaoudi, *J. Am. Chem. Soc.*, 2011, **133**, 14204–14207.

99 Y. Belmabkhout, J. F. Eubank, V. Guillerm, H. Mouttaki and M. Eddaoudi, 2014, submitted.

100 C. G. Carson, K. Hardcastle, J. Schwartz, X. Liu, C. Hoffmann, R. A. Gerhardt and R. Tannenbaum, *Eur. J. Inorg. Chem.*, 2009, 2338–2343.

101 K. Seki, S. Takamizawa and W. Mori, *Chem. Lett.*, 2001, **30**, 332–333.

102 S. Henke, A. Schneemann, A. Wütscher and R. A. Fischer, *J. Am. Chem. Soc.*, 2012, **134**, 9464–9474.



103 R. Kitaura, F. Iwahori, R. Matsuda, S. Kitagawa, Y. Kubota, M. Takata and T. C. Kobayashi, *Inorg. Chem.*, 2004, **43**, 6522–6524.

104 S. Henke, R. Schmid, J.-D. Grunwaldt and R. A. Fischer, *Chem. – Eur. J.*, 2010, **16**, 14296–14306.

105 K. Uemura, Y. Yamasaki, Y. Komagawa, K. Tanaka and H. Kita, *Angew. Chem., Int. Ed.*, 2007, **46**, 6662–6665.

106 K. Uemura, F. Onishi, Y. Yamasaki and H. Kita, *J. Solid State Chem.*, 2009, **182**, 2852–2857.

107 L.-G. Zhu and H.-P. Xiao, *Z. Anorg. Allg. Chem.*, 2008, **634**, 845–847.

108 S. Furukawa, K. Hirai, K. Nakagawa, Y. Takashima, R. Matsuda, T. Tsuruoka, M. Kondo, R. Haruki, D. Tanaka, H. Sakamoto, S. Shimomura, O. Sakata and S. Kitagawa, *Angew. Chem., Int. Ed.*, 2009, **48**, 1766–1770.

109 P. Maniam and N. Stock, *Inorg. Chem.*, 2011, **50**, 5085–5097.

110 J. Y. Lee, D. H. Olson, L. Pan, T. J. Emge and J. Li, *Adv. Funct. Mater.*, 2007, **17**, 1255–1262.

111 Y. Zhao, H. Wu, T. J. Emge, Q. Gong, N. Nijem, Y. J. Chabal, L. Kong, D. C. Langreth, H. Liu, H. Zeng and J. Li, *Chem. – Eur. J.*, 2011, **17**, 5101–5109.

112 K. Hirai, S. Furukawa, M. Kondo, H. Uehara, O. Sakata and S. Kitagawa, *Angew. Chem., Int. Ed.*, 2011, **50**, 8057–8061.

113 H. Chun, D. N. Dybtsev, H. Kim and K. Kim, *Chem. – Eur. J.*, 2005, **11**, 3521–3529.

114 K. Hirai, S. Furukawa, M. Kondo, M. Meilikhov, Y. Sakata, O. Sakata and S. Kitagawa, *Chem. Commun.*, 2012, **48**, 6472–6474.

115 D. Tanaka, S. Horike, S. Kitagawa, M. Ohba, M. Hasegawa, Y. Ozawa and K. Toriumi, *Chem. Commun.*, 2007, 3142–3144.

116 K. Uemura, Y. Yamasaki, F. Onishi, H. Kita and M. Ebihara, *Inorg. Chem.*, 2010, **49**, 10133–10143.

117 Z. Chen, S. Xiang, H. D. Arman, P. Li, D. Zhao and B. Chen, *Eur. J. Inorg. Chem.*, 2011, 2227–2231.

118 H. Kim, D. G. Samsonenko, S. Das, G.-H. Kim, H.-S. Lee, D. N. Dybtsev, E. A. Berdonosova and K. Kim, *Chem. – Asian J.*, 2009, **4**, 886–891.

119 M. Kim, J. A. Boissonnault, P. V. Dau and S. M. Cohen, *Angew. Chem., Int. Ed.*, 2011, **50**, 12193–12196.

120 K. Li, J. Lee, D. H. Olson, T. J. Emge, W. Bi, M. J. Eibling and J. Li, *Chem. Commun.*, 2008, 6123–6125.

121 H. Wang, J. Getzschmann, I. Senkovska and S. Kaskel, *Microporous Mesoporous Mater.*, 2008, **116**, 653–657.

122 D. N. Dybtsev, H. Chun and K. Kim, *Angew. Chem., Int. Ed.*, 2004, **43**, 5033–5036.

123 H. Chun and J. Moon, *Inorg. Chem.*, 2007, **46**, 4371–4373.

124 Z. Chen, S. Xiang, D. Zhao and B. Chen, *Cryst. Growth Des.*, 2009, **9**, 5293–5296.

125 O. Kozachuk, K. Khaletskaya, M. Halbherr, A. Bétard, M. Meilikhov, R. W. Seidel, B. Jee, A. Pöppl and R. A. Fischer, *Eur. J. Inorg. Chem.*, 2012, 1688–1695.

126 M. Kondo, Y. Takashima, J. Seo, S. Kitagawa and S. Furukawa, *CrystEngComm*, 2010, **12**, 2350–2353.

127 N. Klein, C. Herzog, M. Sabo, I. Senkovska, J. Getzschmann, S. Paasch, M. R. Lohe, E. Brunner and S. Kaskel, *Phys. Chem. Chem. Phys.*, 2010, **12**, 11778–11784.

128 K. Kongpatpanich, S. Horike, M. Sugimoto, S. Kitao, M. Seto and S. Kitagawa, *Chem. Commun.*, 2013, **50**, 2292–2294.

129 L.-P. Zhang, J.-F. Ma, J. Yang, Y.-Y. Pang and J.-C. Ma, *Inorg. Chem.*, 2010, **49**, 1535–1550.

130 C. Qin, X. Wang, L. Carlucci, M. Tong, E. Wang, C. Hu and L. Xu, *Chem. Commun.*, 2004, 1876–1877.

131 B. Chen, F. R. Fronczek, B. H. Courtney and F. Zapata, *Cryst. Growth Des.*, 2006, **6**, 825–828.

132 B. Chen, C. Liang, J. Yang, D. S. Contreras, Y. L. Clancy, E. B. Lobkovsky, O. M. Yaghi and S. Dai, *Angew. Chem., Int. Ed.*, 2006, **45**, 1390–1393.

133 S. I. Vagin, A. K. Ott, S. D. Hoffmann, D. Lanzinger and B. Rieger, *Chem. – Eur. J.*, 2009, **15**, 5845–5853.

134 H. He, J. Dou, D. Li, H. Ma and D. Sun, *CrystEngComm*, 2011, **13**, 1509–1517.

135 B.-Q. Ma, K. L. Mulfort and J. T. Hupp, *Inorg. Chem.*, 2005, **44**, 4912–4914.

136 S. Henke, A. Schneemann, S. Kapoor, R. Winter and R. A. Fischer, *J. Mater. Chem.*, 2012, **22**, 909–918.

137 L. Wang, M. Yang, Z. Shi, Y. Chen and S. Feng, *J. Solid State Chem.*, 2005, **178**, 3359–3365.

138 Q. Gao, Y.-B. Xie, J.-R. Li, D.-Q. Yuan, A. A. Yakovenko, J.-H. Sun and H.-C. Zhou, *Cryst. Growth Des.*, 2012, **12**, 281–288.

139 S. W. Lee, H. J. Kim, Y. K. Lee, K. Park, J.-H. Son and Y.-U. Kwon, *Inorg. Chim. Acta*, 2003, **353**, 151–158.

140 P. Kanoo, R. Matsuda, M. Higuchi, S. Kitagawa and T. K. Maji, *Chem. Mater.*, 2009, **21**, 5860–5866.

141 B. Chen, S. Ma, E. J. Hurtado, E. B. Lobkovsky, C. Liang, H. Zhu and S. Dai, *Inorg. Chem.*, 2007, **46**, 8705–8709.

142 H.-J. Hao, F.-J. Liu, H.-F. Su, Z.-H. Wang, D.-F. Wang, R.-B. Huang and L.-S. Zheng, *CrystEngComm*, 2012, **14**, 6726–6731.

143 D. Ma, Y. Li and Z. Li, *Chem. Commun.*, 2011, **47**, 7377–7379.

144 S. Furukawa, K. Hirai, Y. Takashima, K. Nakagawa, M. Kondo, T. Tsuruoka, O. Sakata and S. Kitagawa, *Chem. Commun.*, 2009, 5097–5099.

145 X.-M. Liu, L.-H. Xie, J.-B. Lin, R.-B. Lin, J.-P. Zhang and X.-M. Chen, *Dalton Trans.*, 2011, **40**, 8549–8554.

146 J. Seo, C. Bonneau, R. Matsuda, M. Takata and S. Kitagawa, *J. Am. Chem. Soc.*, 2011, **133**, 9005–9013.

147 Y. Takashima, V. M. Martínez, S. Furukawa, M. Kondo, S. Shimomura, H. Uehara, M. Nakahama, K. Sugimoto and S. Kitagawa, *Nat. Commun.*, 2011, **2**, 168.

148 X.-L. Wang, C. Qin, E.-B. Wang and Z.-M. Su, *Chem. – Eur. J.*, 2006, **12**, 2680–2691.

149 M. Du, Z.-H. Zhang, X.-G. Wang, L.-F. Tang and X.-J. Zhao, *CrystEngComm*, 2008, **10**, 1855–1865.

150 I.-H. Park, K. Kim, S. S. Lee and J. J. Vittal, *Cryst. Growth Des.*, 2012, **12**, 3397–3401.

151 O. K. Farha, K. L. Mulfort, A. M. Thorsness and J. T. Hupp, *J. Am. Chem. Soc.*, 2008, **130**, 8598–8599.

152 A. Modrow, D. Zargarani, R. Herges and N. Stock, *Dalton Trans.*, 2011, **40**, 4217–4222.



153 A. P. Nelson, D. A. Parrish, L. R. Cambrea, L. C. Baldwin, N. J. Trivedi, K. L. Mulfort, O. K. Farha and J. T. Hupp, *Cryst. Growth Des.*, 2009, **9**, 4588–4591.

154 H. Liu, Y. Zhao, Z. Zhang, N. Nijem, Y. J. Chabal, H. Zeng and J. Li, *Adv. Funct. Mater.*, 2011, **21**, 4754–4762.

155 T. Gadzikwa, G. Lu, C. L. Stern, S. R. Wilson, J. T. Hupp and S. T. Nguyen, *Chem. Commun.*, 2008, 5493–5495.

156 B. Chen, S. Ma, F. Zapata, E. B. Lobkovsky and J. Yang, *Inorg. Chem.*, 2006, **45**, 5718–5720.

157 K. L. Mulfort, T. M. Wilson, M. R. Wasielewski and J. T. Hupp, *Langmuir*, 2008, **25**, 503–508.

158 T. Takei, T. Ii, J. Kawashima, T. Ohmura, M. Ichikawa, M. Hosoe, Y. Shinya, I. Kanoya and W. Mori, *Chem. Lett.*, 2007, **36**, 1136–1137.

159 E.-Y. Choi, K. Park, C.-M. Yang, H. Kim, J.-H. Son, S. W. Lee, Y. H. Lee, D. Min and Y.-U. Kwon, *Chem. – Eur. J.*, 2004, **10**, 5535–5540.

160 Z. Fu, J. Yi, Y. Chen, S. Liao, N. Guo, J. Dai, G. Yang, Y. Lian and X. Wu, *Eur. J. Inorg. Chem.*, 2008, 628–634.

161 B. Moulton and M. J. Zaworotko, *Chem. Rev.*, 2001, **101**, 1629–1658.

162 S. Vagin, A. Ott, H.-C. Weiss, A. Karbach, D. Volkmer and B. Rieger, *Eur. J. Inorg. Chem.*, 2008, 2601–2609.

163 S. Subramanian and M. J. Zaworotko, *Angew. Chem., Int. Ed. Engl.*, 1995, **34**, 2127–2129.

164 O. K. Farha, A. M. Shultz, A. A. Sarjeant, S. T. Nguyen and J. T. Hupp, *J. Am. Chem. Soc.*, 2011, **133**, 5652–5655.

165 C. Y. Lee, O. K. Farha, B. J. Hong, A. A. Sarjeant, S. T. Nguyen and J. T. Hupp, *J. Am. Chem. Soc.*, 2011, **133**, 15858–15861.

166 K. L. Mulfort, O. K. Farha, C. D. Malliakas, M. G. Kanatzidis and J. T. Hupp, *Chem. – Eur. J.*, 2010, **16**, 276–281.

167 O. K. Farha, C. D. Malliakas, M. G. Kanatzidis and J. T. Hupp, *J. Am. Chem. Soc.*, 2010, **132**, 950–951.

168 C. Y. Lee, Y.-S. Bae, N. C. Jeong, O. K. Farha, A. A. Sarjeant, C. L. Stern, P. Nickias, R. Q. Snurr, J. T. Hupp and S. T. Nguyen, *J. Am. Chem. Soc.*, 2011, **133**, 5228–5231.

169 T. Gadzikwa, O. K. Farha, C. D. Malliakas, M. G. Kanatzidis, J. T. Hupp and S. T. Nguyen, *J. Am. Chem. Soc.*, 2009, **131**, 13613–13614.

170 T. Gadzikwa, O. K. Farha, K. L. Mulfort, J. T. Hupp and S. T. Nguyen, *Chem. Commun.*, 2009, 3720–3722.

171 K. L. Mulfort, O. K. Farha, C. L. Stern, A. A. Sarjeant and J. T. Hupp, *J. Am. Chem. Soc.*, 2009, **131**, 3866–3867.

172 A. M. Shultz, O. K. Farha, D. Adhikari, A. A. Sarjeant, J. T. Hupp and S. T. Nguyen, *Inorg. Chem.*, 2011, **50**, 3174–3176.

173 A. M. Shultz, O. K. Farha, J. T. Hupp and S. T. Nguyen, *J. Am. Chem. Soc.*, 2009, **131**, 4204–4205.

174 W. Bury, D. Fairen-Jimenez, M. B. Lalonde, R. Q. Snurr, O. K. Farha and J. T. Hupp, *Chem. Mater.*, 2013, **25**, 739–744.

175 S. Takaishi, E. J. DeMarco, M. J. Pellin, O. K. Farha and J. T. Hupp, *Chem. Sci.*, 2013, **4**, 1509–1513.

176 P. M. Barron, H.-T. Son, C. Hu and W. Choe, *Cryst. Growth Des.*, 2009, **9**, 1960–1965.

177 P. M. Barron, C. A. Wray, C. Hu, Z. Guo and W. Choe, *Inorg. Chem.*, 2010, **49**, 10217–10219.

178 B. J. Burnett, P. M. Barron, C. Hu and W. Choe, *J. Am. Chem. Soc.*, 2011, **133**, 9984–9987.

179 E.-Y. Choi, P. M. Barron, R. W. Novotny, H.-T. Son, C. Hu and W. Choe, *Inorg. Chem.*, 2008, **48**, 426–428.

180 H. Chung, P. M. Barron, R. W. Novotny, H.-T. Son, C. Hu and W. Choe, *Cryst. Growth Des.*, 2009, **9**, 3327–3332.

181 M. Bi, G. Li, J. Hua, Y. Liu, X. Liu, Y. Hu, Z. Shi and S. Feng, *Cryst. Growth Des.*, 2007, **7**, 2066–2070.

182 O. M. Yaghi, G. M. Li and H. L. Li, *Nature*, 1995, **378**, 703–706.

183 H. J. Choi and M. P. Suh, *J. Am. Chem. Soc.*, 1998, **120**, 10622–10628.

184 C. J. Kepert, T. J. Prior and M. J. Rosseinsky, *J. Solid State Chem.*, 2000, **152**, 261–270.

185 T. J. Prior, D. Bradshaw, S. J. Teat and M. J. Rosseinsky, *Chem. Commun.*, 2003, 500–501.

186 A. L. Grzesiak, F. J. Uribe, N. W. Ockwig, O. M. Yaghi and A. J. Matzger, *Angew. Chem., Int. Ed.*, 2006, **45**, 2553–2556.

187 C. Gao, S. Liu, L. Xie, Y. Ren, J. Cao and C. Sun, *CrystEngComm*, 2007, **9**, 545–547.

188 S. Jeong, D. Kim, X. Song, M. Choi, N. Park and M. S. Lah, *Chem. Mater.*, 2013, **25**, 1047–1054.

189 S. Jeong, D. Kim, S. Shin, D. Moon, S. J. Cho and M. S. Lah, *Chem. Mater.*, 2014, **26**, 1711–1719.

190 J. X. Chen, M. Ohba and S. Kitagawa, *Chem. Lett.*, 2006, **35**, 526–527.

191 L. Wang, T. Song, C. Li, J. Xia, S. Wang, L. Wang and J. Xu, *J. Solid State Chem.*, 2012, **190**, 208–215.

192 X. Lin, I. Telepeni, A. J. Blake, A. Dailly, C. M. Brown, J. M. Simmons, M. Zoppi, G. S. Walker, K. M. Thomas, T. J. Mays, P. Hubberstey, N. R. Champness and M. Schroeder, *J. Am. Chem. Soc.*, 2009, **131**, 2159–2171.

193 S. Yang, X. Lin, A. Dailly, A. J. Blake, P. Hubberstey, N. R. Champness and M. Schroeder, *Chem. – Eur. J.*, 2009, **15**, 4829–4835.

194 D. Zhao, D. Yuan, A. Yakovenko and H.-C. Zhou, *Chem. Commun.*, 2010, **46**, 4196–4198.

195 Z. Liang, J. Du, L. Sun, J. Xu, Y. Mu, Y. Li, J. Yu and R. Xu, *Inorg. Chem.*, 2013, **52**, 10720–10722.

196 Y. Yan, S. Yang, A. J. Blake and M. Schroeder, *Acc. Chem. Res.*, 2013, **47**, 296–307.

197 X. Duan, J. Yu, J. Cai, Y. He, C. Wu, W. Zhou, T. Yildirim, Z. Zhang, S. Xiang, M. O'Keeffe, B. Chen and G. Qian, *Chem. Commun.*, 2013, **49**, 2043–2045.

198 J. K. Schnobrich, O. Lebel, K. A. Cychosz, A. Dailly, A. G. Wong-Foy and A. J. Matzger, *J. Am. Chem. Soc.*, 2010, **132**, 13941–13948.

199 J. Cai, X. Rao, Y. He, J. Yu, C. Wu, W. Zhou, T. Yildirim, B. Chen and G. Qian, *Chem. Commun.*, 2014, **50**, 1552–1554.

200 S. Yang, X. Lin, A. J. Blake, K. M. Thomas, P. Hubberstey, N. R. Champness and M. Schroeder, *Chem. Commun.*, 2008, 6108–6110.



201 S. Yang, X. Lin, A. J. Blake, G. S. Walker, P. Hubberstey, N. R. Champness and M. Schroeder, *Nat. Chem.*, 2009, **1**, 487–493.

202 S. Yang, S. K. Callear, A. J. Ramirez-Cuesta, W. I. F. David, J. Sun, A. J. Blake, N. R. Champness and M. Schroeder, *Faraday Discuss.*, 2011, **151**, 19–36.

203 S. Yang, G. S. B. Martin, J. J. Titman, A. J. Blake, D. R. Allan, N. R. Champness and M. Schroeder, *Inorg. Chem.*, 2011, **50**, 9374–9384.

204 Z.-J. Lin, L.-W. Han, D.-S. Wu, Y.-B. Huang and R. Cao, *Cryst. Growth Des.*, 2012, **13**, 255–263.

205 Y. Zou, C. Yu, Y. Li and M. S. Lah, *CrystEngComm*, 2012, **14**, 7174–7177.

206 Z.-J. Lin, T.-F. Liu, Y.-B. Huang, J. Lü and R. Cao, *Chem. – Eur. J.*, 2012, **18**, 7896–7902.

207 J. J. Perry, G. J. McManus and M. J. Zaworotko, *Chem. Commun.*, 2004, 2534–2535.

208 H. Abourahma, G. J. Bodwell, J. J. Lu, B. Moulton, I. R. Pottie, R. B. Walsh and M. J. Zaworotko, *Cryst. Growth Des.*, 2003, **3**, 513–519.

209 J. F. Eubank, L. Wojtas, M. R. Hight, T. Bousquet, V. C. Kravtsov and M. Eddaoudi, *J. Am. Chem. Soc.*, 2011, **133**, 17532–17535.

210 M. O'Keeffe, M. Eddaoudi, H. L. Li, T. M. Reineke and O. M. Yaghi, *J. Solid State Chem.*, 2000, **152**, 3–20.

211 S. Xiang, J. Huang, L. Li, J. Zhang, L. Jiang, X. Kuang and C.-Y. Su, *Inorg. Chem.*, 2011, **50**, 1743–1748.

212 L. Du, Z. Lu, K. Zheng, J. Wang, X. Zheng, Y. Pan, X. You and J. Bai, *J. Am. Chem. Soc.*, 2012, **135**, 562–565.

213 X. Liu, M. Oh and M. S. Lah, *Inorg. Chem.*, 2011, **50**, 5044–5053.

214 X. Liu, M. Oh and M. S. Lah, *Cryst. Growth Des.*, 2011, **11**, 5064–5071.

215 Y.-S. Wei, R.-B. Lin, P. Wang, P.-Q. Liao, C.-T. He, W. Xue, L. Hou, W.-X. Zhang, J.-P. Zhang and X.-M. Chen, *CrystEngComm*, 2014, **16**, 6325–6330.

216 S. S. Y. Chui, S. M. F. Lo, J. P. H. Charmant, A. G. Orpen and I. D. Williams, *Science*, 1999, **283**, 1148–1150.

217 X.-S. Wang, S. Ma, D. Sun, S. Parkin and H.-C. Zhou, *J. Am. Chem. Soc.*, 2006, **128**, 16474–16475.

218 S. Ma, D. Sun, M. Ambrogio, J. A. Fillinger, S. Parkin and H.-C. Zhou, *J. Am. Chem. Soc.*, 2007, **129**, 1858–1859.

219 Z. Zhang, L. Zhang, L. Wojtas, M. Eddaoudi and M. J. Zaworotko, *J. Am. Chem. Soc.*, 2012, **134**, 928–933.

220 Y. Inokuma, S. Yoshioka, J. Ariyoshi, T. Arai, Y. Hitora, K. Takada, S. Matsunaga, K. Rissanen and M. Fujita, *Nature*, 2013, **495**, 461–462.

221 X.-S. Wang, S. Ma, D. Yuan, J. W. Yoon, Y. K. Hwang, J.-S. Chang, X. Wang, M. R. Jorgensen, Y.-S. Chen and H.-C. Zhou, *Inorg. Chem.*, 2009, **48**, 7519–7521.

222 H. Furukawa, Y. B. Go, N. Ko, Y. K. Park, F. J. Uribe-Romo, J. Kim, M. O'Keeffe and O. M. Yaghi, *Inorg. Chem.*, 2011, **50**, 9147–9152.

223 G.-Q. Kong, Z.-D. Han, Y. He, S. Ou, W. Zhou, T. Yildirim, R. Krishna, C. Zou, B. Chen and C.-D. Wu, *Chem. – Eur. J.*, 2013, **19**, 14886–14894.

224 W. Lu, D. Yuan, T. A. Makal, J.-R. Li and H.-C. Zhou, *Angew. Chem., Int. Ed.*, 2012, **51**, 1580–1584.

225 Z. Wei, W. Lu, H.-L. Jiang and H.-C. Zhou, *Inorg. Chem.*, 2013, **52**, 1164–1166.

226 N. B. Shustova, A. F. Cozzolino and M. Dincă, *J. Am. Chem. Soc.*, 2012, **134**, 19596–19599.

227 X.-L. Yang, M.-H. Xie, C. Zou, Y. He, B. Chen, M. O'Keeffe and C.-D. Wu, *J. Am. Chem. Soc.*, 2012, **134**, 10638–10645.

228 L. Ma, D. J. Mihalcik and W. Lin, *J. Am. Chem. Soc.*, 2009, **131**, 4610–4612.

229 C. Tan, S. Yang, N. R. Champness, X. Lin, A. J. Blake, W. Lewis and M. Schroeder, *Chem. Commun.*, 2011, **47**, 4487–4489.

230 Z.-J. Lin, T.-F. Liu, X.-L. Zhao, J. Lü and R. Cao, *Cryst. Growth Des.*, 2011, **11**, 4284–4287.

231 B. F. Abrahams, S. R. Batten, H. Hamit, B. F. Hoskins and R. Robson, *Angew. Chem., Int. Ed. Engl.*, 1996, **35**, 1690–1692.

232 Q. Zhang, Y. Liu, X. Bu, T. Wu and P. Feng, *Angew. Chem., Int. Ed.*, 2008, **47**, 113–116.

233 X. Zhao, H. He, T. Hu, F. Dai and D. Sun, *Inorg. Chem.*, 2009, **48**, 8057–8059.

234 Z.-Z. Xue, T.-L. Sheng, Q.-L. Zhu, D.-Q. Yuan, Y.-L. Wang, C.-H. Tan, S.-M. Hu, Y.-H. Wen, Y. Wang, R.-B. Fu and X.-T. Wu, *CrystEngComm*, 2013, **15**, 8139–8145.

235 Z.-M. Hao, C.-H. Guo, H.-S. Wu and X.-M. Zhang, *CrystEngComm*, 2010, **12**, 55–58.

236 T. E. Gier, X. Bu, S.-L. Wang and G. D. Stucky, *J. Am. Chem. Soc.*, 1996, **118**, 3039–3040.

237 Z.-J. Lin, Y.-B. Huang, T.-F. Liu, X.-Y. Li and R. Cao, *Inorg. Chem.*, 2013, **52**, 3127–3132.

238 Y.-S. Xue, Y. He, L. Zhou, F.-J. Chen, Y. Xu, H.-B. Du, X.-Z. You and B. Chen, *J. Mater. Chem. A*, 2013, **1**, 4525–4530.

239 B. Nohra, H. El Moll, L. M. Rodriguez Albelo, P. Mialane, J. Marrot, C. Mellot-Draznieks, M. O'Keeffe, R. Ngo Biboum, J. Lemaire, B. Keita, L. Nadjo and A. Dolbecq, *J. Am. Chem. Soc.*, 2011, **133**, 13363–13374.

240 M. Eddaoudi, Unpublished results.

241 A. G. Wong-Foy, O. Lebel and A. J. Matzger, *J. Am. Chem. Soc.*, 2007, **129**, 15740–15741.

242 C.-S. Lim, J. K. Schnobrich, A. G. Wong-Foy and A. J. Matzger, *Inorg. Chem.*, 2010, **49**, 5271–5275.

243 A. Schoedel, W. Boyette, L. Wojtas, M. Eddaoudi and M. J. Zaworotko, *J. Am. Chem. Soc.*, 2013, **135**, 14016–14019.

